Geological Survey of Finland
Circular Economy Solutions Unit
Vuorimiehentie 2K
Espoo Finland

December 11, 2023 GTK/884/03.01/2020
Open File Work Report
86/2023

Towards creating a set of Battery Mineral Reference Materials
for Applied Mineralogy and Mineral Processing Research

Part 2: Lithium Reference Materials

By

Alan R Butcher
Professor of Geomaterials & Applied Mineralogy, GTK, Finland

With contributions from

Lorenza Sardisco[#], Nikolaos Apeiranthitis[$], Maximilian Franzel[$], Johanna Tepsell[+] and Tim J Pearce[+$]

[+]X-ray Mineral Services Oy (XMSF), [#]X-ray Mineral Services Ltd (UK) & [$]Hafren Scientific Group

GTK Open File Work Report

Geologian tutkimuskeskus | Geologiska forskningscentralen | Geological Survey of Finland
Espoo • Kokkola • Kuopio • Loppi • Outokumpu • Rovaniemi
www.gtk.fi • Puh/Tel +358 29 503 0000 • Y-tunnus / FO-nummer / Business ID: 0244680-7

December 11, 2023

GEOLOGICAL SURVEY OF FINLAND **DOCUMENTATION PAGE**

11 December 2023

Authors Butcher et al	Type of report GTK Open File Work Report
	Commissioned by Business Finland
Title of report Towards creating a set of Battery Mineral Reference Materials for Applied Mineralogy and Mineral Processing Research **Part 2: Lithium Reference Materials**	
Abstract See Summary	
Keywords Reference Material, battery minerals, drill core, lithium minerals, QXRD, SEM-EDS, ICP-OES, ICP-MS, Raman, LIBS, FTIR	
Other information This report is deliverable D5.3.1(b) of the BATCircle2.0 Project, funded by Business Finland	
Report serial GTK Open File Work Report	Archive code 86/2023
Total pages 41 / Language English	Price NA / Confidentiality Public
Unit Circular Economy Solutions	Project code 50404-40210210
Name/signature Jouko Nieminen Head of Unit	Signature/name Alan R Butcher Research Professor

December 11, 2023

Contents

PAGE

December 11, 2023

Summary

This study documents the geochemical and mineralogical characteristics of several **Lithium Reference Materials**, and forms part of **Work Package 5**, Circular Battery Materials Value System, as part of **BATCircle2.0 Project**, in collaboration with partners **Aalto University** and **VTT**. This is **Part 2** of four deliverables, with others covering similar reports on Nickel and Cobalt Reference Materials, along with recommendations for an e-Waste Reference Material.

The new **Reference Materials** reported here comprise **spodumene**- and **petalite**-bearing samples, some of which (those from Keliber) are marked as potential lithium ores of the future.

Together, they are not designed to be definitive mineral or rock standards, but rather represent samples that have been characterized using multiple methods (optical, e-beam, x-ray beam, laser-beam), at different scales (cm-micron), and in different forms (drill core, crushed and milled ore, thin-section, polished block).

It is the intention that the new data and physical sub-samples will be made available to all those within the **BATCircle2.0 Consortium** who are interested in battery mineral research. Typical end-users for the new materials might include geologists, mineralogists and material scientists interested in testing new analytical or experimental devices; or minerals engineers that require well-characterized materials for flotation, leaching or physical separation experiments.

A novel aspect of the study is that we have used both traditional geoanalytical techniques for battery mineral characterization (whole rock geochemistry, QXRD, SEM-EDS, EPMA, Automated Mineralogy), as well as new and emerging technologies (scanning micro-XRF, LIBS, FTIR, Raman), thus creating a unqiue set of data for the three sample types, including new spectral information which can be used for building mineral identification libraries. Some of the devices used are handheld and are sufficiently portable that they can be operated efficiently in the field, which opens-up the possibility of wider use, leading to new applications in earth and mineral sciences.

The results, whether they be chemical, mineral or textural in nature, largely correlate across the different techniques. This report aims only to document the findings rather than interpret them or compare them to previous work (published or unpublished), as this activity will form the basis of a planned scientific journal paper in 2024, which will compare the relative accuracy and precision of the results across all 4 commodities (Ni-Li-Co-eWaste).

A further planned output from the present study is a quick reference **Fact Sheet** that will accompany each **Reference Material** before they are dispatched to researchers. This will be published separately once the materials are ready for release.

December 11, 2023

1 CONTEXT

This report summarises research carried out to date by the **Geological Survey of Finland** (**GTK**), within Work Package 5 (**WP5**), Circular Battery Materials Value System, as part of an on-going **Business Finland**-funded Project, known as **BATCircle2.0**, in collaboration with partners **Aalto University** and **VTT**. The specific and relevant objectives of **WP5** are as follows:

- Extensive characterization of battery materials from both **Primary** and **Secondary** sources
- Development of **Reference Materials** for **Li**, **Co** and **Ni**
- Assessment of how to develop an **e-waste** materials characterization reference material

In order to fulfill these objectives, the following tasks are underway:

- **Task 5.3.1**
  Development of **Reference Materials** for **Nickel**, **Lithium** and **Cobalt**

- **Task 5.3.2**
  Assessment to plan the development of characterization of **Reference Electronic Waste**

Four reports are planned, each covering one of the main topics within Tasks 5.3.1 and 5.3.2. The present report documents the results for new **Lithium Reference Materials**, and is labelled accordingly as **Part 2** (of 4).

2 CONCEPT

The original idea was to create a collection of well-characterized materials that could be used by researchers, whether they be geologists, mineralogists, geochemists, mineral processors, or any other professions linked to battery minerals, metals and materials. Ideally, we wanted to characterize ores (drill cores or hand samples, or run-of mine material), processed products (concentrates), and final materials (saleable products), and make sub-samples of these available to all those interested, along with a fact sheet.

3 STANDARD REFERENCE MATERIAL VS REFERENCE MATERIAL

At the commencement of the **BATCircle2.0 Proje**ct, we wanted to clarify the meaning of the following terms, Standard, Standard Reference Material, and Reference Material.

A **Standard** is generally defined (at least in the world of analytical geomaterials) as a material (say crystal, mineral, rock type) with absolute known values that can be used for calibrating analytical techniques & instrumentation. It is usually available in the form of a fine powder, or a single crystal or

grain, which tends to limit the variability of the standard from sub-sample to sub-sample during manufacture.

On the other hand, a **Standard Reference Material** (again, in the context of analytical geomaterials) is a general term for a so-called *round-robin* material, which is specifically manufactured to be analysed by multiple laboratories in order to establish intra- and inter-laboratory variation, in terms of accuracy, precision, and general variance in results, especially when comparing the same technology (say ICP or XRF), or different technologies (say XRD, SEM and EPMA).

Our preferred terminology, and the one used in the present study, is simply to refer to these types of materials in this study as **Reference Materials**. By using this short descriptor, we imply that materials have been specifically created with scientific and engineering research in mind. These **Reference Materials**, although well-characterized (in terms of their bulk geochemical composition, known mineral content and textures, and other material properties), will display natural variation, from batch to batch, because of their very nature (drill cores, ore lumps, and processed mineral particles), and so cannot be considered as true **Standards**.

Multiple batches of **Reference Material** will be manufactured as aliquots from a Master sample, and made available, in the first instance at least, to members of the **BATCircle2.0 Consortium**, and then later to interested parties outside, depending on demand and availability of material. Each batch will be accompanied by a **Fact Sheet**, which we believe will be adequate to allow the recipient to plan and design their own experiments, and is certainly an excellent starting point for any further research on them. Ideally, additional analytical work on these batches would then be fed back to the GTK and incorporated into documentation of any future batches. The kinds of uses we envisage for these **Reference Materials** might include, but are not restricted to, the following: teaching, research, professional development, fingerprinting (tracking and tracing), general metallurgical testing, and technology testing.

4 GEOANALYTICAL TECHNIQUES USED TO CHARACTERIZE THE REFERENCE MATERIALS

There are a bewildering number of analytical techniques that are currently available to geologists when it comes to the characterization of drill cores, crushed core and particulate mineral products. These include: optical methods (petrographic microscopy); X-ray analysis (XRF, XRD, X-CT), electron-beam analysis (SEM, EPMA) and laser-based techniques (LA-ICP-MS, Raman, LIBS) and others (FTIR).

In the present report, we document many of these for a suite of **Lithium-bearing Reference Materials** sampled from various deposits in Finland (see **Table 1** below) have been characterized using the META multidisciplinary geomaterial workflow developed by X-ray Mineral Services (XMS UK) to explore various Mineralogical, Elemental and Textural Analyses (META) to provide cross-validated analytical data. Specifically, the “gold-standard” techniques of XRD, ICP-OES/MS, Automated Mineralogy (AMICS), and Raman spectroscopy were used to characterise the samples, with cross-calibration against a portable technique, FTIR.

5 DETAIL OF THE MASTER SAMPLES USED TO MAKE THE LITHIUM REFERENCE MATERIALS

Lithium-bearing mineral rock samples from different localities in Finland were selected as potential sources for Lithium Reference Materials:

- **Hirvikallio** – Petalite
- **Kaustinen** – Spodumene Green variety (**Syväjärvi**)
- **Kaustinen** – Spodumene Pink variety (**Länttä**)
- **Kietyönmäki** – Spodumene

The table below summarises the analytical activities on each sample.

Table 1. Analytical schedule

		b=bulk, c=crystal, h=hand					
	Sample Ref	**XRD**	**ICP**	**Li ICP**	**FTIR**	**Raman**	**AMICS**
Petalite - Hirvikallio, Finland							
Hirvi 1.b	PHB-1					x	x
	PHB-2					x	
	PHB	x +cy	x	x	x		
Hirvi Petalite 1	PHC1	x	x	x	x		
Hirvi Petalite 2	PHC2	x	x	x	x		
Hirvi Petalite 3	PHC3	x wrc		x	x		
Hirvi Petalite 4	PHC4	x	x	x	x		
Hirvi Petalite 4.c	PHH	x	x	x	x		
						x	x
Spodumene - Kaustinen, Finland							
Green							
Keliber Oy Syvajarvi Pilot 2019	SS19B	x +cy	x	x	x		
						x	x
	SS19C	x	x	x	x		
Keliber Oy Syvajarvi November 202	SS21B-1					x	x
	SS21B-2					x	
	SS21B-3					x	
	SS21B	x +cy	x	x	x		
	SS21C	x	x	x	x		
Pink							
Keliber Oy Lantta November 2021	SL21B-1					x	x
	SL21B-2					x	
	SL21B	x +cy	x	x	x		
	SL21C	x	x	x	x		
Spodumene - Kietyonmaki, Finland May 2023							
Kiety 1.b	SK23B					x	x
	SK23B	x +cy	x	x	x		

6 CHARACTERIZATION OF THE LITHIUM REFERENCE MATERIALS

X-ray Fluorescence Spectrometry (**XRF**) is a standard method of analysis in order to gain a bulk geochemical analysis of any geomaterial. It is ideal for major elements, some minor elements, but is generally unsuitable for trace and ultra-trace elements, such lithium. The sample is typically required to be in the form of pressed powdered pellets or glass beads.

Inductively Coupled Plasma Optical Emission spectroscopy (**ICP-OES**) is generally considered a superior method for multi-elemental analysis over XRF, for both major and minor elements, but is only suitable for some trace elements.

Inductively Coupled Plasma Mass Spectrometry (**ICP-MS**) is used typically only for trace elements, and can analyse, if required, down to detection limits of parts per billion. It is especially useful for quantifying rare earth elements.

X-ray diffraction is a robust whole-rock analytical technique for identifying minerals and phases present in a sample, based on their characteristic diffraction patterns, and when used in conjunction with specialised software, the **Rietveld method** allows for quantitative modal analysis (**XRD**). Minerals present in low quantities (5 vol% or less) can be problematic for XRD. Some minerals display overlapping diffractograms, leading to challenging identifications. The technique relies on the ability to determine the crystallinity of the mineral for a positive identification to be made, and therefore amorphous minerals are therefore problematic. Sample needs to be pulverized to a fine powder.

Automated Mineralogy is an established method to map 2D polished surface of samples by Scanning Electron Microcopy using Energy Dispersive Spectrometry (**SEM-EDS**) to determine micro-composition, and to create mineral maps with textural details that allow for quantification of grain sizes, shapes and associations. Grain boundaries, inclusions, and fractures can also be mapped. The sample is usually presented to the instrument in the form of a thin section or polished block. Scanning resolution can be down to as little as 1 micron, but typically a stepping interval greater than this is used to speed up measurement time.

Raman spectroscopy (**Raman**) is a non-destructive mineral analysis technique which provides detailed information about chemical structure, phase identification and crystallinity. It is based upon the interaction of light with the chemical bonds within a material, following interaction with a laser beam focused onto the surface of a sample.

Fourier Transform Infra-Red spectroscopy (**FTIR**) uses a monochromatic beam of light and measures how much of the light is absorbed, and the algorithm used to calculate this (taking raw data and making it into a spectrum that can be interpreted for mineralogical information) is known as the Fourier Transform. It was used in this study as an experimental method.

Laser Induced Breakdown Spectroscopy (**LIBS**) is a technology gaining momentum in the mining industry after having much success in the oil and gas sector. The laser is focussed to form a plasma which atomizes and excites the sample under investigation. Typically used in field portable devices. Certain elements found in particular minerals respond well to LIBS, such as Li in spodumene. It was not specifically used in this study as it is still considered an experimental method, but on-going research at GTK suggests it shows great promise.

7 TECHNICAL INFORMATION FOR LITHIUM REFERENCE MATERIALS

7.1 Whole-rock multi-element geochemical analysis - ICP-OES, ICP-MS

ICP-OES and **ICP-MS** analysis was undertaken at the X-Ray Services Ltd Welshpool lab by Lithium Metaborate Fusion following the method presented in Finlay et al. (2023), except lithium which was determined with ICP-OES using the $HF/HClO_4$ acid digestion method at the University of Greenwich, UK (Jarvis & Jarvis 1992a).

Inductively-coupled plasma – optical emission spectrometry (**ICP-OES**) involves the analysis of the optical spectra produced by samples as they pass into an excitation source or high temperature plasma. Inductively-coupled plasma – mass spectrometry (**ICP-MS**) utilises a similar plasma excitation source, but instead of viewing the optical spectra, it passes the emission into a mass spectrometer for analysis. Both instruments analyse samples in solution, therefore all solid samples need to be dissolved prior to analysis.

All samples were ground to a fine powder in agate mortars. Following preparation, the samples were prepared for ICP analyses by using the lithium metaborate (alkali) fusion procedure, as advocated by Jarvis & Jarvis (1992a and 1992b). The flux was mixed with the sample in a carbon crucible with a 5:1 ratio and heated to 1050°C in a muffle furnace. The molten bead was then tipped into dilute nitric acid (2%) and allowed to dissolve. The chemical composition of the dissolved samples were determined using a Thermo iCAP 7000 ICP-OES and Thermo iCAP RQ ICP-MS instruments, with quantitative data being acquired for forty-eight elements, which include ten major elements, e.g., Al, Si, Ti, Fe, Mn, Mg, Ca, Na, K and P, twenty-four trace elements, e.g., Ba, Be, Co, Cr, Cs, Cu, Ga, Hf, Mo, Nb, Ni, Pb, Rb, Sc, Sr, Ta, Tl, Th, U, V, W, Y, Zn and Zr, and fourteen rare earth elements, e.g., La, Ce, Pr, Nd, Sm, Eu, Gd, Tb, Dy, Ho, Er, Tm, Yb and Lu. The precision of the geochemical data acquired by the ICP analyses is determined by replicate analyses of multiple preparations of certified rock standard reference materials (SRMs), along with duplicate preparations of three unknown samples, which are analysed on a routine basis along with each of the samples. With reference to the SRMs, the absolute accuracy of all the data are generally considered to lie within the range of error achieved for multi-determinations of the same sample.

7.2 XRD - Mineralogical analysis

X-Ray diffraction (**XRD**) is an analytical technique used for the quantitative determination of minerals present in crystalline material such as rocks. The method depends upon the unique structural properties of the analysed crystals and measures the intensities and scattering of the x-rays leaving the sample.

13 samples were selected for XRD, details of which are provided in Table 1. All samples were prepared and analysed at X-ray Mineral Services Ltd, Colwyn Bay, UK.

7.2.1 Whole-rock XRD

The samples were first disaggregated gently using a pestle and mortar. A 2 g split of this material was micronized in water using a McCrone Micronising Mill. The gentle size reduction process used by this mill preserves the crystal lattice of the sample producing a powder with a mean particle diameter of 5 - 10 microns. The slurry was dried overnight at 80°C, re-crushed to a fine powder and back-packed into a steel

sample holder, producing a randomly orientated powder for presentation to the x-ray beam. Whole-rock samples were scanned on a PANalytical X'Pert3 diffractometer using a CuKα radiation at 40 kV and 40 mA. The diffractometer is equipped with Automatic Divergence Slits (10 mm irradiated area), sample spinner and PIXcel 1-D detector. Whole rock samples were scanned from 4.5 to 75° (2θ) at a step size of 0.013 for 2 hours. The longer scan time improves the resolution of the data, which is particularly important for detecting Li-bearing minerals.

The goal of the whole rock sample preparation is to have a random orientation of the grains, allowing unbiased phase quantification and minimizing the error caused by preferred orientation of certain minerals (e.g. mica flakes, feldspar, calcite).

7.2.2 Clay Fraction XRD

Although clay minerals may be evident in whole rock diffractograms, the most satisfactory method for their identification is to extract and analyse the clay fraction separately. A 5 g split of the sample that was disaggregated at the first stage of the whole rock preparation (see above) was weighed accurately. The weight was recorded in a central register for later reference. Separating the <2-micron fraction was achieved by ultrasound and centrifugation. The total weight of clay extracted was determined by removing a 20-25 g aliquot of the final clay suspension and evaporating to dryness at 80°C. The initial and final weights of the beaker used were also recorded in the register.

The clay XRD mount was obtained by filtering the clay suspension through a Millipore glass micro-fibre filter and drying the filtrate on the filter paper. The samples were analysed as an untreated clay, after saturation with ethylene glycol vapour overnight and following heating at 380°C for 2 hours, with a further heating to 550°C for one hour.

The clay filters were scanned on a Philips PW1730 Generator with a CuKα radiation at 40 kV and 40 mA. from 3 to 35° (2θ) at a step size of 0.05° and 2 s step time.

7.2.3 XRD Interpretation

The qualitative analysis of whole rock diffractograms to Identify the minerals present was carried out using two commercial software packages associated with the ICDD database: Traces (v.6) by GBC Scientific Equipment and HighScore Plus (v.4) by PANalytical. Identification and characterization of clay minerals in the <2-micron fraction was performed following the guidelines described by Moore and Reynolds (1997) and overlaying the diffractograms from the four clay treatments.

Whole rock quantification

For this study, XRD quantitative phase analysis on whole rock samples was performed using the Rietveld method with BGMN AutoQuan software. The Rietveld method is based upon a full-pattern analysis (rather than single peaks) where a computer model allows a theoretical diffractogram to be calculated for any phase mixture. For further details on the application of this method for quantitative phase analysis, refer to Post and Bish (1989). An independent in-house normalized Reference Intensity Ratio (RIR) method was also used to verify the phase quantification. This is a single line RIR method that has been calibrated for the instrument present at X-ray Mineral Services with more than a hundred pure or semi-pure minerals.

Clay fraction quantification

Clay quantification was performed on the samples using a Reference Intensity Ratio based method whereby the peak intensities are measured and incorporated in a formula to indicate the relative amounts of clay minerals present. This data is then used to quantify the clay minerals with respect to the whole rock by reference to the total amount of <2-micron fraction, which is calculated from the aliquot previously extracted and dried. An indication of the clay minerals crystallinity was given by assessment of the peak width for each component.

7.3 Automated SEM-EDS Analysis

Six samples were prepared and investigated by Helford Geoscience LLP using automated SEM-EDS analysis to quantify the phases present (see **Table 2** below).

Table 2. Samples analysed by Automated Mineralogy

Sample Number	Description
PHB-1	Petalite Hirvikallio Finland. Hirvi 1.b bulk sample.
PHH	Petalite Hirvikallio Finland. Hirvi petalite 4c.
SS19B	Green spodumene, Kaustinen, Finland. Keliber Oy Syväjärvi Pilot 2019.
SS21B-1	Green spodumene, Kaustinen, Finland. Keliber Oy Syväjärvi Nov 21.
SL21B-1	Pink spodumene, Kaustinen, Finland. Keliber Oy Länttä Nov 21.
SK23B	Spodumene, Kietyönmäki, Finland, May 23. Kiety 1.b.

AMICS is an acronym for Automated Mineral Identification and Characterization System by Bruker. This technology brings together a high-resolution BSE imaging (back scattered electron) with a high-throughput EDS (energy dispersive spectrometer) for a solution that automates the collection of data from the Scanning Electron Microscope (SEM) and provides tools for the identification of phases (mineral or synthetic). The technique provides a quantitative breakdown of sample mineralogy along with key textural information in a spatially resolved sample map. AMICS is the next generation characterization tool for detailed and quantitative analysis of samples incorporating innovative imaging and analysis.

7.3.1 Sample preparation

The surface of the samples had been previously polished, and the mineralogy examined using RAMAN spectroscopy (Figure 1). The samples were digitally photographed and then re-polished, carbon coated and measured directly, so that the AMICS mineral analysis is based on the same surface as examined by RAMAN spectroscopy.

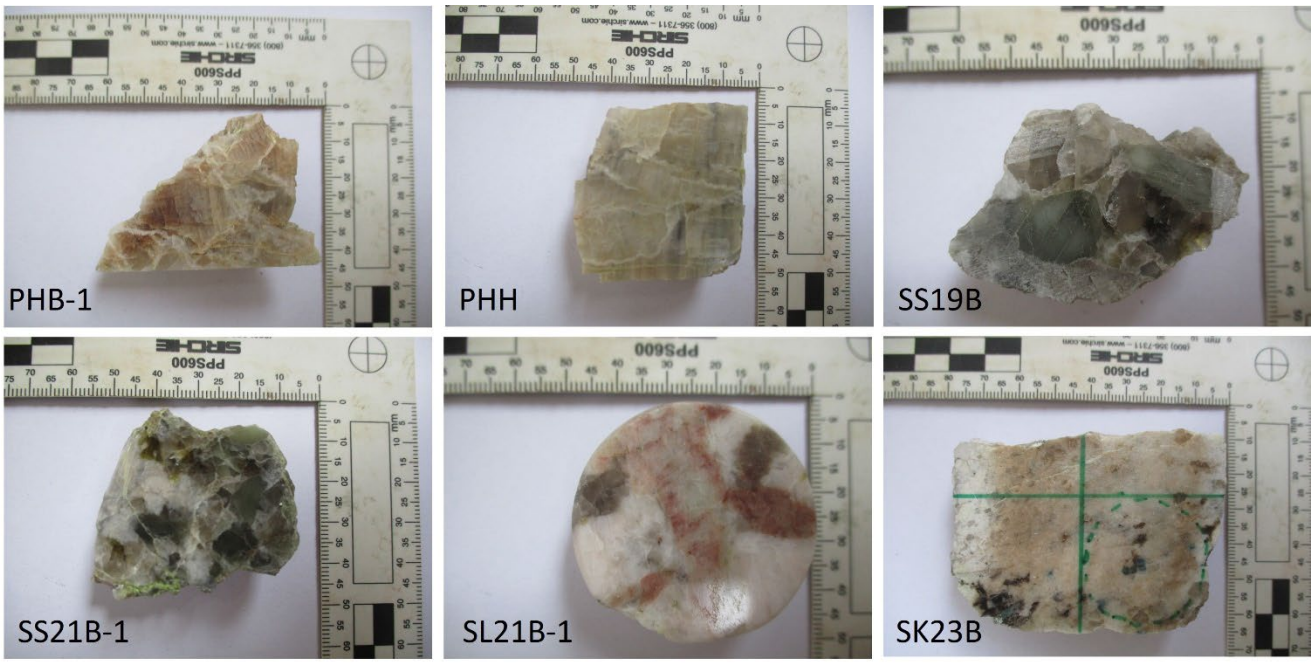

Figure 1. Samples submitted for AMICS mineral analysis.

The mineralogy and texture of the sample was quantified through automated SEM-EDS mineral analysis (Schultz et al., 2020). Analysis was undertaken using a Hitachi SU3900 scanning electron microscope fitted with two large area (60 mm²) Bruker SDD energy dispersive spectrometers and running the AMICS automated mineralogy software package. Beam conditions were optimised for analysis and therefore an accelerating voltage of 20kV coupled with a beam current of approximately 15 nA were used. The sample was measured with a segmented field image mode of analysis. This analytical mode subdivides the BSE image into domains (segments) of similar brightness which represent different mineral grains / crystals and then acquires a representative EDS X-ray spectrum from a point within the segment; the mineral identified is then assigned to the entire segment. Measurements were optimised to highlight both textural and modal mineralogical information and a resolution of 5 µm was achieved.

The EDS spectra acquired during the measurement are compared with a library of measured and synthetic standards and a mineral identification is made on a closest match basis. Phases which are not represented in the standards list at the time of measurement are added either by acquiring reference spectra directly from the sample, or by creating a reference spectrum from the measurement itself. As the standards list can comprise hundreds of reference spectra, the data are grouped into a final, reported mineral list (**Table 6**). It should be noted that the samples had previously been polished using Al powder, which may be present ingrained into fractures in the surface; the possible presence of this Al has been considered during the data processing. Modal data expressed as both area % and mass % are provided. During the Automated Mineralogy analysis full area SEM-BSE montages are also captured of the analysed areas.

7.4 Raman Spectroscopy

Raman spectroscopy is an automated mineral identification technique that is based upon inelastic scattering of light when a sample is irradiated with a laser (Raman-effect). It is used to characterise the chemistry and structure of a grain/crystal to identify the mineral, and can also provide information on texture, size, liberation and relationships between phases. The technology is routinely used to quantify the accessory mineral composition in sandstones or coarse silt to sand sized materials. The effective constraint on analysis is the grain-size of the analyte. Also, in this project it was used on rocks to construct mineralogy maps for further analysis. For interpreting the Raman data, database Raman shift spectra were taken from the RRUFF database as well as the literature available on some of the phases present in the samples analysed.

Raman analysis has been done on polished rock chips, as shown in Figure 1. A high-resolution acquisition map pattern was configured within the Raman controlling software, for over 20000 spectra per sample. The total acquisition time for each sample reached 12-13 hours, with following the spectra processing, spectral matching, and map construction, with in-house software, reaching at 24 hours per sample. The result of this analysis is shown in the results where all the acquisition specifications are included in the figures.

For this study, 10 samples were analysed, the same as for AMICS, (but a different surface to that used for Raman analysis), and a comparison is made to help understand the capabilities of both techniques.

7.5 Fourier Transform Infrared Spectroscopy (FTIR)

For the FTIR analysis, 12 samples out of the total 13 were analysed for acquiring mid-infrared (M-IR) spectra, PHB, PHC1, PHC2, PHC4, PHH, SS19B, SS19C, SS21B, SS21C, SL21B, SL21C, SK23B, as indicated in **Table 1**.

Fourier Transform Infrared Spectroscopy (**FTIR**) is a technique used to obtain an infrared spectrum from a broad spectral range. The technology is used to detect different functional groups with characteristic absorption or emission lines. FTIR can provide mineralogical data as percentage with minimal sample requirements from small sample volumes when based on a model built from XRD data.

The samples were run on the same split as the XRD analyses to ensure that the FTIR results are comparable to the XRD results. The samples were analysed with a compact Bruker Alpha FTIR spectrometer which is first set-up to collect a background spectrum with a clear sample plate. Once this is collected, approximately 50 mg of the powdered sample is put on the sample window and analysed. The instrument then calculates and presents the spectrum.

Upon data collection, the different vibrating bands of the spectrum are qualitatively assigned to the structures / stretching and bending vibrations of molecules that are expected to be present, based on the XRD results, e.g., Si-O for silicates, CO_3 for carbonates, Al-O for aluminosilicates. For mono-mineralogical samples, database FTIR spectra are compared with the sample spectra, which can lead to identification of structural interferences due to cations substituting key structural sites of the minerals. Although these changes are not unique to one or two substitutions, the chemical breakdown of those samples can be indicative of these changes.

The FTIR range is used for the analysis of the samples is from 4000 cm^{-1} to 400 cm^{-1}, 32 scans with a spectral resolution of 4 cm^{-1}.

8. RESULTS

8.1 ICP-OES and ICP-MS

A general summary of the geochemical results is provided in **Table 3**, with specific details for lithium recorded in Table 3a.

Table 3. ICP-OES and ICP-MS data

			Petalite - Hirvikallio					Spodumene - Kaustinen						Spod Kietyönmäki	
								Keliber Oy Syvajarvi Pilot 2019 - Green		Keliber Oy Syvajarvi Nov 2021 - Green		Keliber Oy Länttä Nov 2021 - Pink		Kiety 1.b	
			PHB	PHC1	PHC2	PHC3	PHC4	PHH	SS19B	SS19C	SS21B	SS21C	SL21B	SL21C	
	Method		Bulk Sample	Crystal 1	Crystal 2	Crystal 3	Crystal 4	Hirvi Petalite 4.c	Bulk Sample	Crystal	Bulk Sample	Crystal	Bulk Sample	Crystal	
Li	ICP-OES	ppm	15210	15600	16305	19645	19875	16280	5995	15460	10590	17725	5265	8590	1022
Al2O3	ICP-OES	%	16.38	17.00	15.90		16.11	16.41	15.95	18.35	16.46	19.34	15.54	11.95	17.30
SiO2	ICP-OES	%	77.56	75.57	76.19		77.06	78.02	72.81	74.09	76.56	69.93	74.07	82.04	70.22
TiO2	ICP-OES	%	0.01	0.01	0.01		0.00	0.01	0.10	0.03	0.02	0.02	0.01	0.01	0.01
Fe2O3	ICP-OES	%	0.17	0.20	0.11		0.22	0.39	0.89	0.63	0.46	0.81	0.28	0.47	0.10
MnO	ICP-OES	%	0.02	0.01	0.01		0.01	0.02	0.07	0.07	0.08	0.21	0.08	0.10	0.02
MgO	ICP-OES	%	0.06	0.07	0.05		0.08	0.08	0.33	0.09	0.08	0.15	0.11	0.26	0.07
CaO	ICP-OES	%	0.24	0.13	0.14		0.13	0.42	0.89	0.27	0.55	0.92	0.28	0.19	0.68
Na2O	ICP-OES	%	2.37	1.15	1.51		0.11	1.26	3.66	1.79	3.44	0.97	4.82	1.37	9.41
K2O	ICP-OES	%	0.21	1.12	0.13		0.07	0.38	2.97	0.92	0.93	1.98	2.00	0.84	0.36
P2O5	ICP-OES	%	0.15	0.04	0.05		0.01	0.22	0.54	0.17	0.43	0.77	0.06	0.02	0.41
S	ICP-OES	mg/kg	338.73	192.72	203.17		641.99	264.48	417.31	296.96	360.36	554.68	142.17	70.53	0.00
Be	ICP-MS	mg/kg	59.72	12.27	6.69		14.41	7.61	182.50	172.13	193.34	13.29	341.33	18.38	243.75
Sc	ICP-OES	mg/kg	0.20	0.64	0.23		0.03	0.51	2.05	0.63	0.54	0.41	0.06	0.04	0.88
V	ICP-MS	mg/kg	1.61	1.93	1.52		2.24	2.54	12.99	2.24	2.39	3.81	1.61	1.73	1.39
Cr	ICP-MS	mg/kg	1.92	1.47	3.82		1.05	1.08	41.28	12.81	3.83	1.44	2.36	0.81	1.14
Co	ICP-MS	mg/kg	0.73	0.80	0.83		0.57	1.22	1.93	0.61	0.96	0.95	0.59	0.61	0.62
Ni	ICP-MS	mg/kg	3.74	3.85	3.30		2.33	2.86	6.13	1.75	2.81	2.07	3.07	3.05	3.93
Cu	ICP-MS	mg/kg	4.90	3.88	3.73		4.75	3.95	12.62	5.29	32.29	5.82	3.43	3.44	3.19
Zn	ICP-MS	mg/kg	25.42	23.14	46.40		17.56	50.18	52.73	70.01	40.26	68.15	104.39	91.54	9.80
Ga	ICP-MS	mg/kg	20.87	26.70	19.31		15.83	20.89	26.17	39.04	26.47	34.06	45.85	46.42	27.62
Rb	ICP-MS	mg/kg	51.43	403.74	26.75		8.98	130.08	508.20	192.39	163.82	327.24	476.05	166.57	52.91
Sr	ICP-MS	mg/kg	4.51	6.96	1.57		1.66	5.87	54.18	12.68	21.78	60.56	12.93	11.30	69.34
Y	ICP-MS	mg/kg	0.57	0.47	11.29		0.25	13.89	118.74	35.55	46.69	1.30	0.24	0.29	0.37
Zr	ICP-MS	mg/kg	5.32	8.52	22.61		3.41	10.44	281.05	73.74	15.88	15.85	9.57	4.44	26.73
Nb	ICP-MS	mg/kg	17.42	20.48	5.51		1.64	28.10	24.26	19.15	16.77	30.82	173.99	19.46	208.22
Mo	ICP-MS	mg/kg	0.14	0.45	0.63		1.15	1.02	1.14	0.13	0.16	0.25	0.32	0.09	0.30
Sn	ICP-MS	mg/kg	25.17	32.18	78.09		5.25	51.26	43.55	105.19	57.42	99.66	11.33	15.29	779.75
Cs	ICP-MS	mg/kg	10.64	27.26	7.70		5.82	12.25	50.04	23.30	20.38	23.77	42.38	16.23	45.29
Ba	ICP-MS	mg/kg	21.08	35.19	13.74		14.28	41.88	59.46	38.20	42.14	128.89	51.97	69.93	15.32
La	ICP-MS	mg/kg	0.60	0.63	55.52		0.42	20.99	602.98	184.36	239.17	9.74	0.59	0.69	0.88
Ce	ICP-MS	mg/kg	1.35	1.50	118.24		1.12	37.38	1299.85	394.34	493.76	22.01	1.34	1.56	1.88
Pr	ICP-MS	mg/kg	0.13	0.16	14.15		0.10	3.85	156.91	47.69	58.09	2.45	0.13	0.16	0.17
Nd	ICP-MS	mg/kg	0.47	0.57	51.28		0.35	13.09	573.63	172.77	205.10	7.45	0.43	0.59	0.50
Sm	ICP-MS	mg/kg	0.09	0.09	8.90		0.06	2.11	98.07	29.97	32.32	1.04	0.08	0.13	0.08
Eu	ICP-MS	mg/kg	0.02	0.04	0.19		0.02	0.23	2.15	0.73	0.74	0.22	0.02	0.03	0.06
Gd	ICP-MS	mg/kg	0.12	0.11	6.81		0.06	2.43	76.96	23.44	26.33	0.80	0.06	0.08	0.09
Tb	ICP-MS	mg/kg	0.02	0.02	0.76		0.01	0.36	8.67	2.59	2.99	0.07	0.01	0.02	0.01
Dy	ICP-MS	mg/kg	0.09	0.08	2.83		0.03	2.01	30.39	9.21	11.18	0.26	0.05	0.04	0.06
Ho	ICP-MS	mg/kg	0.01	0.02	0.41		0.01	0.46	4.60	1.38	1.85	0.04	0.01	0.01	0.01
Er	ICP-MS	mg/kg	0.04	0.03	0.93		0.03	1.26	10.16	3.04	3.94	0.11	0.02	0.02	0.03
Tm	ICP-MS	mg/kg	0.01	0.01	0.09		0.01	0.22	0.88	0.27	0.31	0.02	0.01	0.01	0.01
Yb	ICP-MS	mg/kg	0.03	0.03	0.48		0.03	1.16	5.18	1.61	1.54	0.10	0.02	0.02	0.06
Lu	ICP-MS	mg/kg	0.00	0.01	0.07		0.00	0.18	0.68	0.21	0.18	0.01	0.00	0.00	0.01
Hf	ICP-MS	mg/kg	0.35	0.64	0.78		0.10	0.56	8.46	2.68	1.11	0.97	1.25	0.43	4.39
Ta	ICP-MS	mg/kg	11.63	12.25	13.59		1.05	16.96	14.98	5.67	9.80	7.12	67.14	7.52	351.38
W	ICP-MS	mg/kg	1.76	3.12	2.03		1.18	2.10	1.89	1.78	1.24	0.81	2.14	1.06	3.97
Tl	ICP-MS	mg/kg	0.19	1.32	0.13		0.07	0.49	2.86	0.92	0.87	1.97	3.41	1.01	0.26
Pb	ICP-MS	mg/kg	1.78	2.51	1.70		1.17	1.44	16.00	4.33	8.24	9.53	7.23	1.90	5.43
Th	ICP-MS	mg/kg	0.32	0.37	35.20		0.34	1.81	395.08	120.45	166.79	3.97	3.09	0.47	1.17
U	ICP-MS	mg/kg	3.72	1.08	2.55		2.00	3.96	27.44	9.75	10.74	9.01	8.75	3.74	8.96

Table 3a. ICP-OES data for lithium only, expressed in parts per million

	Sample	ID	Type	Li
			Method	ICP-OES
				ppm
Petalite - Hirvikallio, Finland		PHB	Bulk Sample	15210
		PHC1	Crystal 1	15600
		PHC2	Crystal 2	16305
		PHC3	Crystal 3	19645
		PHC4	Crystal 4	19875
		PHH	Hirvi Petalite 4.c	16280
Spodumene - Kaustinen, Finland	Keliber Oy Syvajarvi Pilot 2019	SS19B	Bulk Sample	5995
	Green	SS19C	Crystal	15460
	Keliber Oy Syvajarvi November 2021	SS21B	Bulk Sample	10590
	Green	SS21C	Crystal	17725
	Keliber Oy Lantta November 2021	SL21B	Bulk Sample	5265
	Pink	SL21C	Crystal	8590
Spodumene - Kietyonmaki, Finland May 2023	Kiety 1.b	SK23B	Bulk Sample	1022

8.2 XRD

Whole-rock results

XRD results for each sample are presented as weight percent (wt %) in **Table 4**.

Petalite, albite and quartz comprise bulk of the mineralogy of the **Hirvikallio** petalite samples together with lesser spodumene, muscovite, smectite and trace amount of chlorite.

Kaustinen spodumene samples are composed mainly of spodumene with variable amounts of quartz, muscovite and albite. Small amounts of beryl are present in most of samples. An unquantifiable trace of chlorite is present in all **Kaustinen** samples except for sample SL21C which shows 2.3% of chlorite.

Kietyönmäki spodumene sample is dominated by albite and quartz with minor muscovite, spodumene, beryl and an unquantifiable trace of apatite.

Clay fraction results

Table 5 shows the semi-quantitative clay XRD results for each sample. The clay fraction preparation includes a measurement for each sample of the total weight of clay that comprises the <2-micron fraction (i.e., wt.% <2µm). The results include %A for each clay species and is derived from the interpretation of the XRD clay data for each sample and in every case will therefore total 100%. The %B is %A for each species multiplied (as a percentage) by the clay weight fraction (i.e., wt.% <2µm). The %B data is then fed back into the 'whole rock' data when a clay species has not been detected in whole rock analysis, which is often the case for mixed-layer clays.

Table 4. Quantitative XRD mineralogy of the whole-rock samples.

	Petalite - Hirvikallio						Spodumene - Kaustinen						Spod Kietyönmäki
							Keliber Oy Syvajarvi Pilot 2019 - Green		Keliber Oy Syvajarvi Nov 2021 - Green		Keliber Oy Länttä Nov 2021 - Pink		Kiety 1.b
ID	PHB	PHC1	PHC2	PHC3	PHC4	PHH	SS19B	SS19C	SS21B	SS21C	SL21B	SL21C	SK23B
Type	Bulk Sample	Crystal 1	Crystal 2	Crystal 3	Crystal 4	Hirvi Petalite 4.c	Bulk Sample	Crystal	Bulk Sample	Crystal	Bulk Sample	Crystal	Bulk Sample
Smectite	0.5	0.0	0.0	1.1	0.0	0.0	0.0	0.0	0.0	0.0	0.0	0.0	0.0
Muscovite	2.8	7.9	2.5	0.0	0.0	5.3	7.4	9.4	5.1	5.1	5.1	5.2	3.2
Kaolinite	0.0	0.0	0.0	0.0	0.0	0.0	0.0	0.0	0.0	0.0	0.0	0.0	0.0
Chlorite	TR	TR	TR	TR	0.0	TR	TR	TR	TR	TR	TR	2.3	0.0
Quartz	14.8	12.5	17.9	7.3	4.1	19.6	31.6	35.2	37.2	26.4	31.1	60.0	14.7
K Feldspar	0.0	4.1	0.0	0.0	0.0	0.0	12.6	TR	TR	9.8	8.9	TR	0.0
Albite	18.8	8.1	11.6	0.0	0.9	8.5	33.5	16.6	29.7	9.1	42.5	12.1	77.3
Spodumene	4.4	3.4	9.8	0.0	0.0	7.7	14.0	38.5	27.9	49.5	12.1	20.3	4.4
Amphibole	0.0	0.0	0.0	0.0	0.0	0.0	0.8	0.0	0.0	0.0	0.0	0.0	0.0
Beryl	0.0	0.0	0.0	0.0	0.0	0.0	0.1	0.3	0.2	0.0	0.3	0.0	0.4
Petalite	58.6	63.9	58.2	91.7	95.0	58.9	0.0	0.0	0.0	0.0	0.0	0.0	0.0
Apatite	0.0	0.0	0.0	0.0	0.0	0.0	0.0	0.0	TR	TR	0.0	0.0	TR
Total	100.0	100.0	100.0	100.0	100.0	100.0	100.0	100.0	100.0	100.0	100.0	100.0	100.0

Table 5. Semi-quantitative XRD mineralogy of the clay fraction samples.

		Petalite - Hirvikallio					Spodumene - Kaustinen						Spod Kietyönmäki	
							Keliber Oy Syvajarvi Pilot 2019 - Green		Keliber Oy Syvajarvi Nov 2021 - Green		Keliber Oy Länttä Nov 2021 - Pink		Kiety 1.b	
	ID	PHB	PHC1	PHC2	PHC3	PHC4	PHH	SS19B	SS19C	SS21B	SS21C	SL21B	SL21C	
		Bulk Sample	Crystal 1	Crystal 2	Crystal 3	Crystal 4	Hirvi Petalite 4.c	Bulk Sample	Crystal	Bulk Sample	Crystal	Bulk Sample	Crystal	
	Wt. % <2um	2.0						2.1		2.2		2.1		1.7
Smectite	% A	24.7						0.0		0.0		0.0		0.0
	% B	0.5						0.0		0.0		0.0		0.0
	Crys	P												
Mica	% A	42.2						69.9		60.3		68.7		39.5
	% B	0.8						1.4		1.4		1.4		0.7
	Order													
Kaolinite	% A	0.0						0.0		0.0		0.0		0.0
	% B	0.0						0.0		0.0		0.0		0.0
	Crys													
Chlorite	% A	TR						0.0		0.0		0.0		0.0
	% B	TR						0.0		0.0		0.0		0.0
	Crys	P												
Quartz	% A	3.5						9.6		13.1		7.3		6.0
	% B	0.1						0.2		0.3		0.2		0.1
Petalite	% A	20.2						0.0		0.0		0.0		0.0
	% B	0.4						0.0		0.0		0.0		0.0
Plagioclase	% A	9.5						16.4		20.3		19.3		42.0
	% B	0.2						0.3		0.5		0.4		0.7
Spodumene	% A	0.0						4.1		6.3		4.7		12.5
	% B	0.0						0.1		0.1		0.1		0.2

8.3 Automated SEM-EDS (AMICS)

The modal mineralogy data are presented in **Table 6**; the data are presented as area %. In this summary the area % data are presented as major minerals (>10%), minor minerals (1-10%) and trace minerals (<1%). Further Automated AMICS images and SEM-BSE images are provided below and in the **Appendix**.

Table 6. Quantitative mineralogy based on Automated Mineralogy.

Sample Name	PHB-1	PHH	SS19B	SS21B-1	SL21B-1	SK23B
Quartz	8.84	6.50	49.19	42.94	10.15	7.24
K Feldspar	0.05	0.07	0.11	6.22	11.73	1.11
Plagioclase	0.50	2.06	2.17	21.06	27.73	84.79
Muscovite	0.24	0.34	9.23	4.96	1.93	3.84
Biotite	0.00	0.00	0.00	0.00	0.00	0.00
Chlorite	0.07	0.11	0.33	0.33	3.63	0.14
Kaolinite	0.09	0.11	0.07	0.10	0.08	0.01
Spodumene	8.61	5.33	37.87	22.95	41.01	0.26
Petalite	80.86	84.85	0.27	0.16	0.37	0.04
Beryl	0.00	0.00	0.00	0.10	0.00	0.81
Eucryptite	0.34	0.28	0.24	0.29	3.07	0.15
Fe Phosphate	0.00	0.00	0.00	0.06	0.00	0.00
Carbonate	0.00	0.00	0.00	0.00	0.00	0.00
Fe Oxides	0.00	0.00	0.00	0.00	0.00	0.00
Apatite	0.01	0.02	0.10	0.44	0.06	1.45
Ti Minerals	0.00	0.00	0.00	0.00	0.00	0.00
Pyrite	0.00	0.00	0.00	0.00	0.00	0.00
Zircon	0.00	0.00	0.00	0.00	0.01	0.01
Barite	0.00	0.00	0.00	0.00	0.00	0.00
Undifferentiated	0.38	0.33	0.42	0.37	0.23	0.17
Total	100.00	100.00	100.00	100.00	100.00	100.00

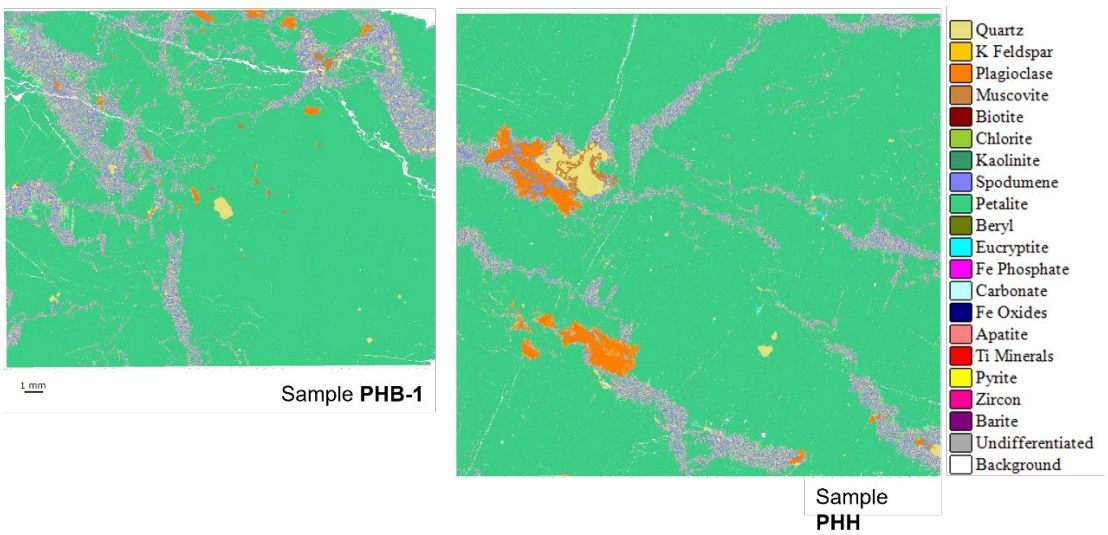

Figure 2. AMICS images for the petalite samples analysed from the Hirvikallio area.

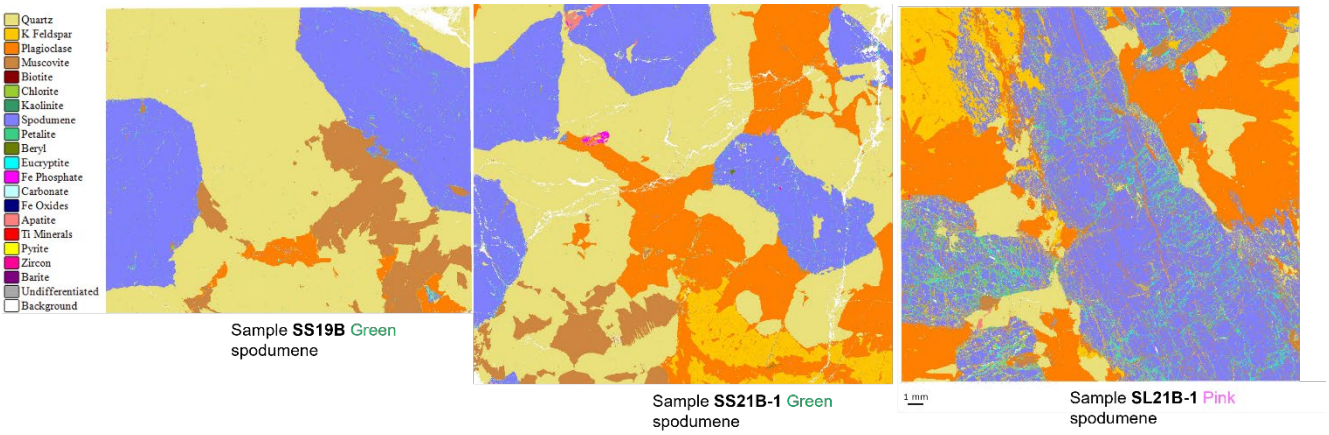

Figure 3. AMICS images for the three spodumene samples analysed from the Kaustinen area.

8.4 Raman Spectroscopy

The Raman mineral identification and mapping worked very well in characterising this spodumene, petalite- and albite-rich samples provided. The in-house developed workflow provided direct identification of these Li-bearing minerals, of spodumene and petalite, with the potential of Li-bearing albite (needs verification with external technique). It was also successful in distinguishing these three minerals, although they are very close in ,chemical composition, as they belong in the solid-solution series of quartz – petalite – (lithium) feldspar – spodumene – eucryptite (Hatch, 1943).

The inherent map resolution is at 150 µm which is dependent on the laser spot size. However, microtextural characteristics that involved the coexistence (intergrowth) of spodumene, and quartz was able to be qualitatively determined with the spectra. An example of that is sample **PHB-1** which shows this microtexture. In the legend of that figure (**Figure 4**) a spodumene/quartz phase was qualitatively identified by the Raman spectra generated. Similarly, the **PHH** petalite sample also shows this in Figure 3. All other textural relations of mineral phases can be appreciated in **Figures 5-9**, as well as compared with AMICS data.

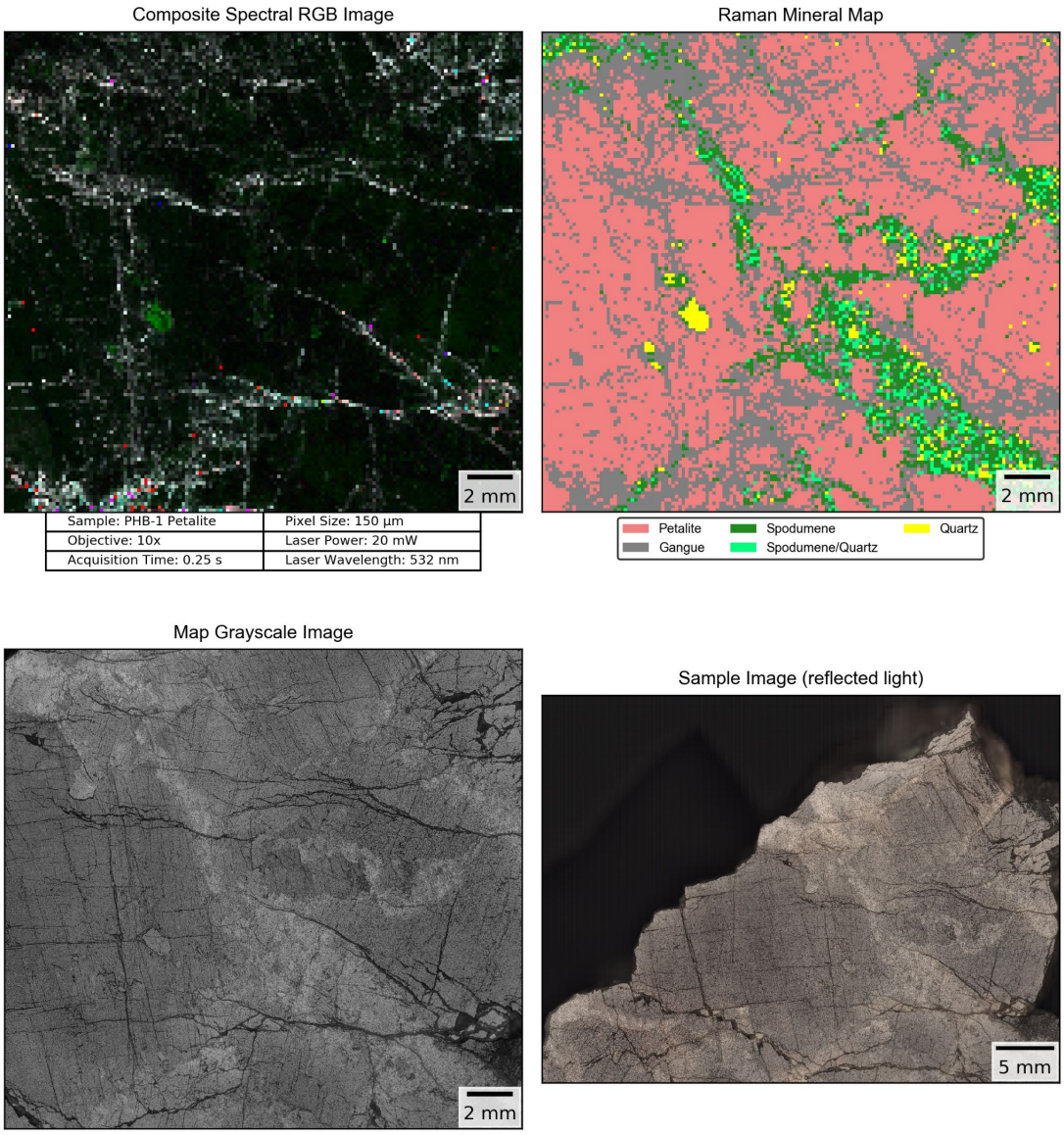

Figure 4. Raman analysis of sample **PHB-1** petalite.

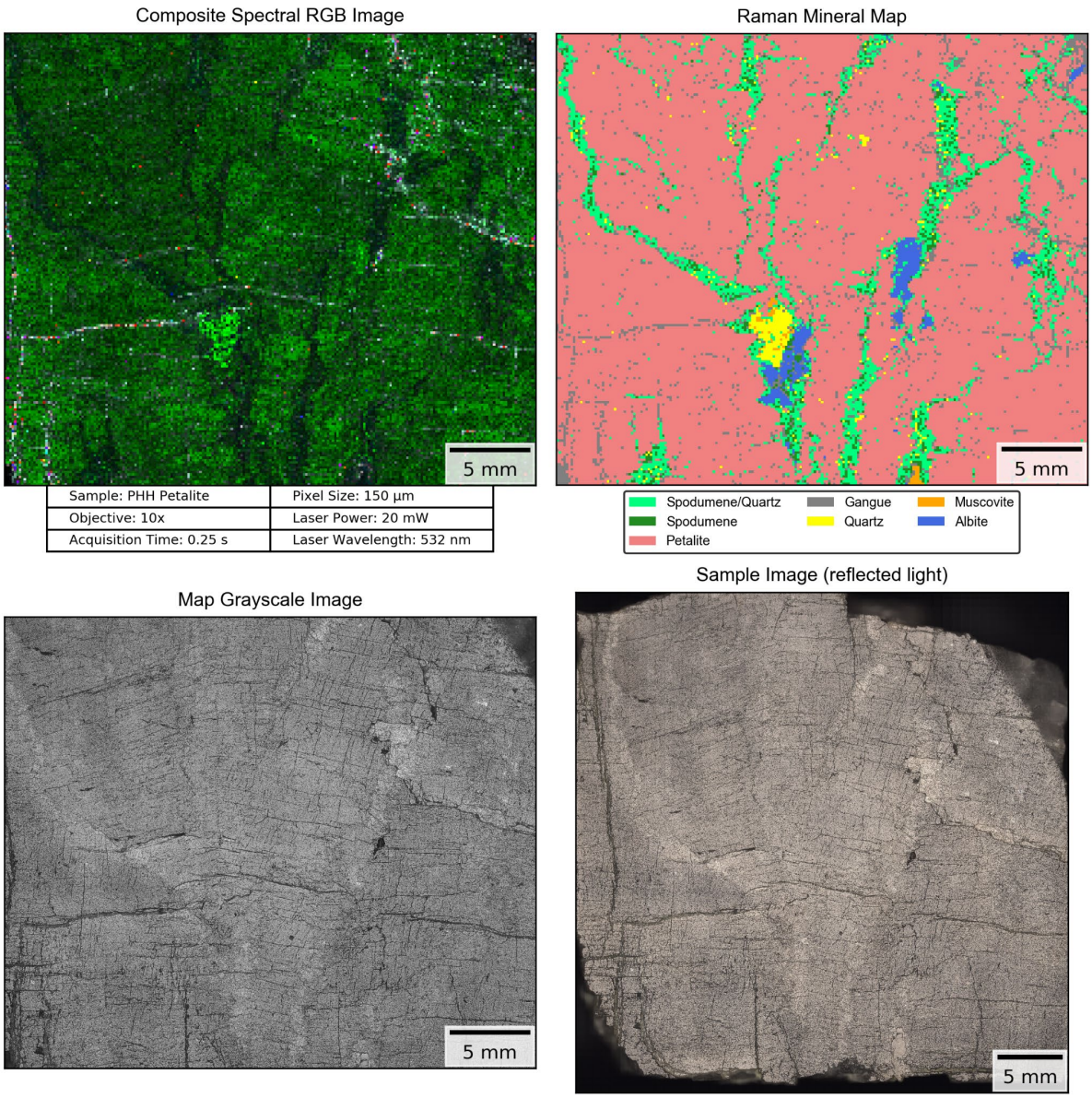

Figure 5. Raman analysis of sample **PHH** petalite

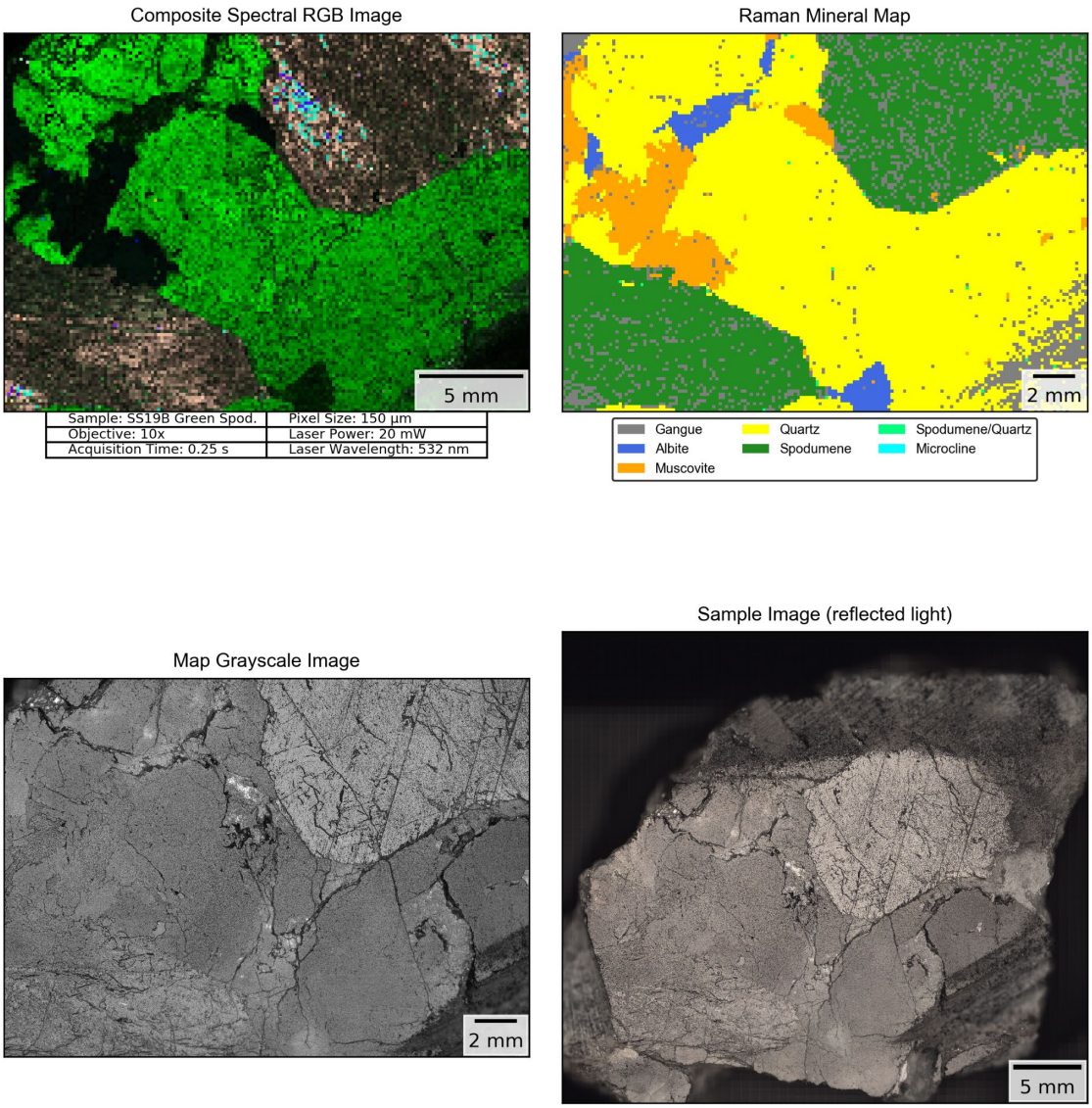

Figure 6. Raman analysis of sample **SS19B** spodumene

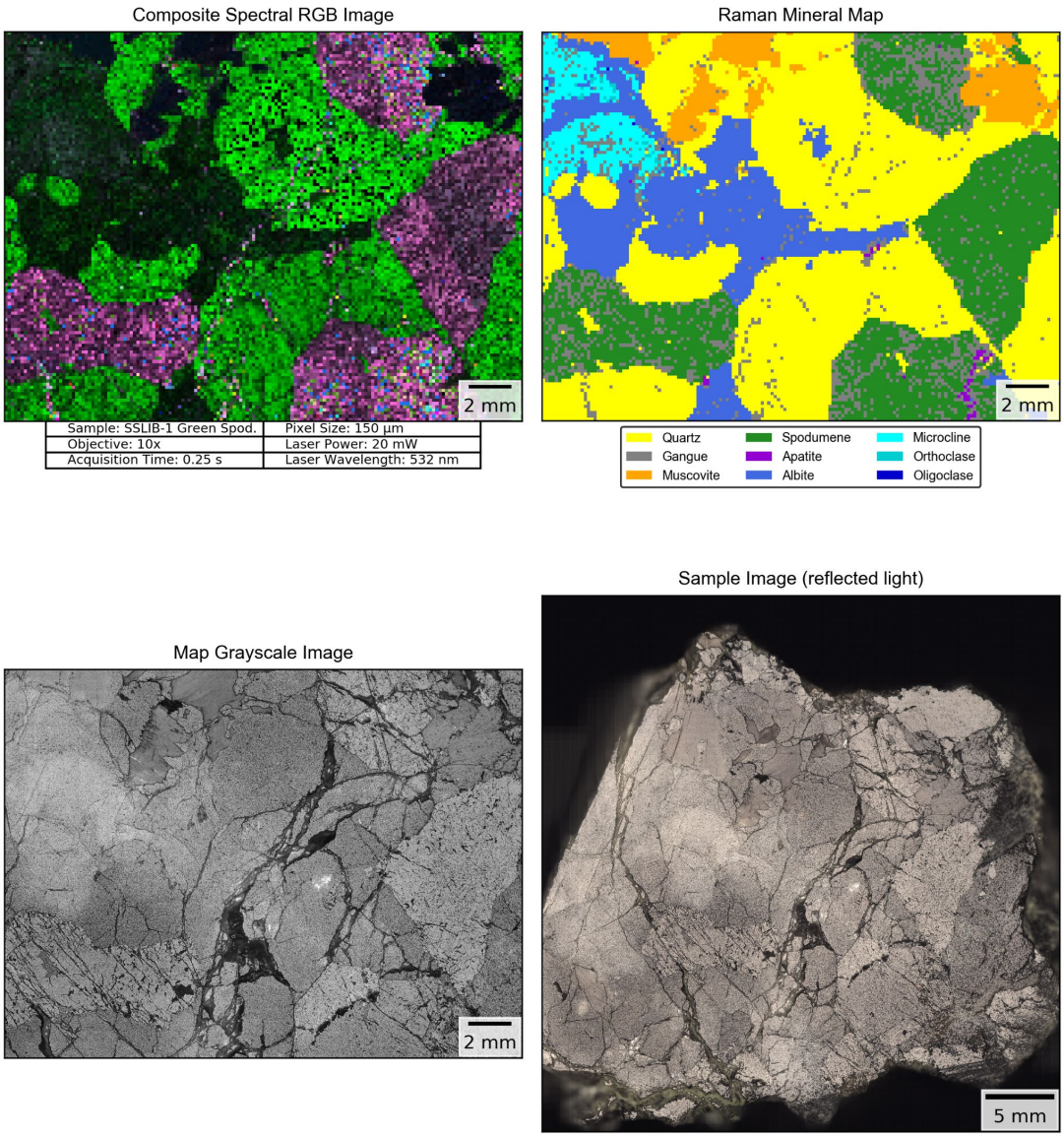

Figure 7. Raman analysis of sample **SSLB-1** spodumene.

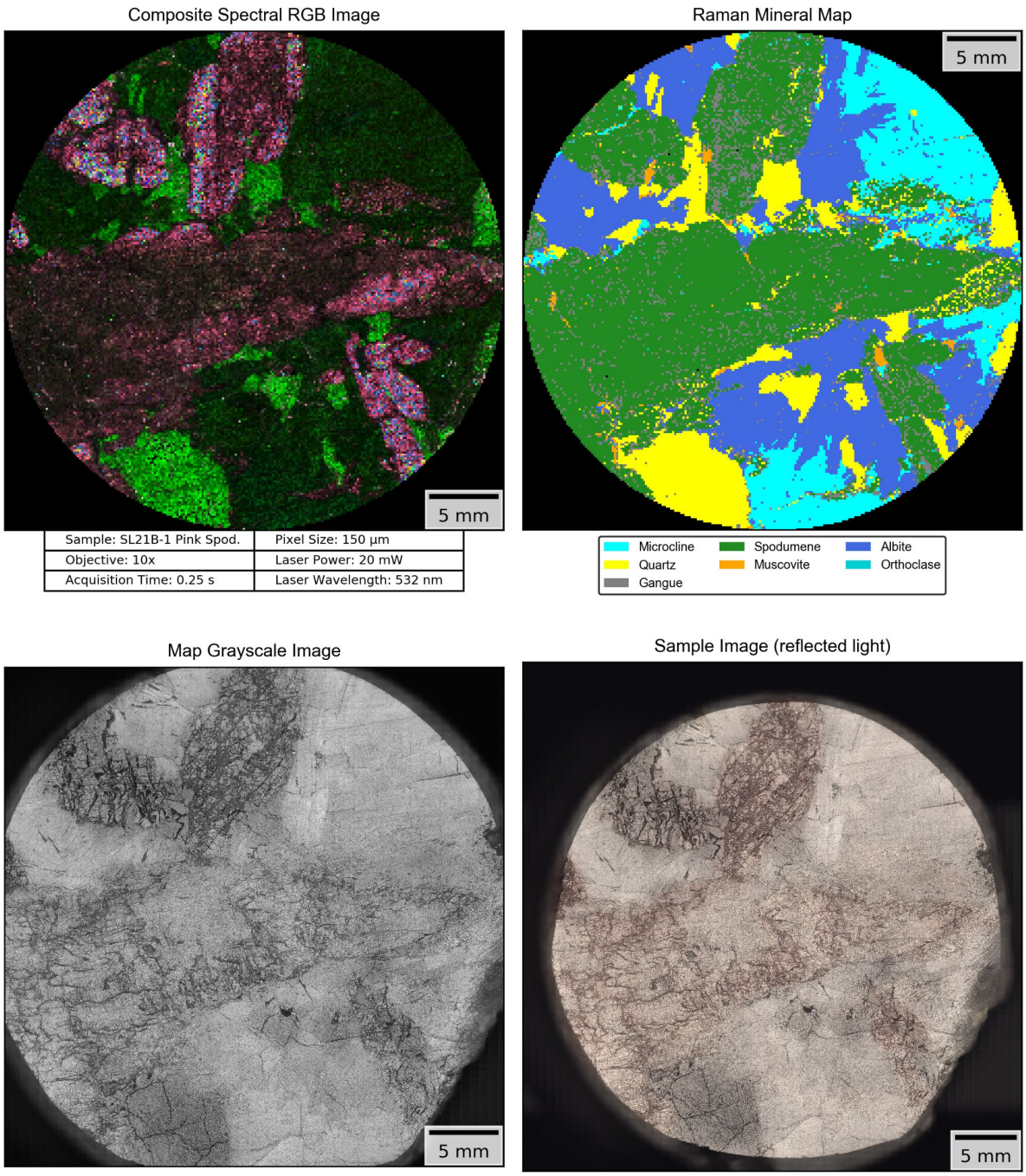

Figure 8. Raman analysis of sample **SL21B** spodumene**.**

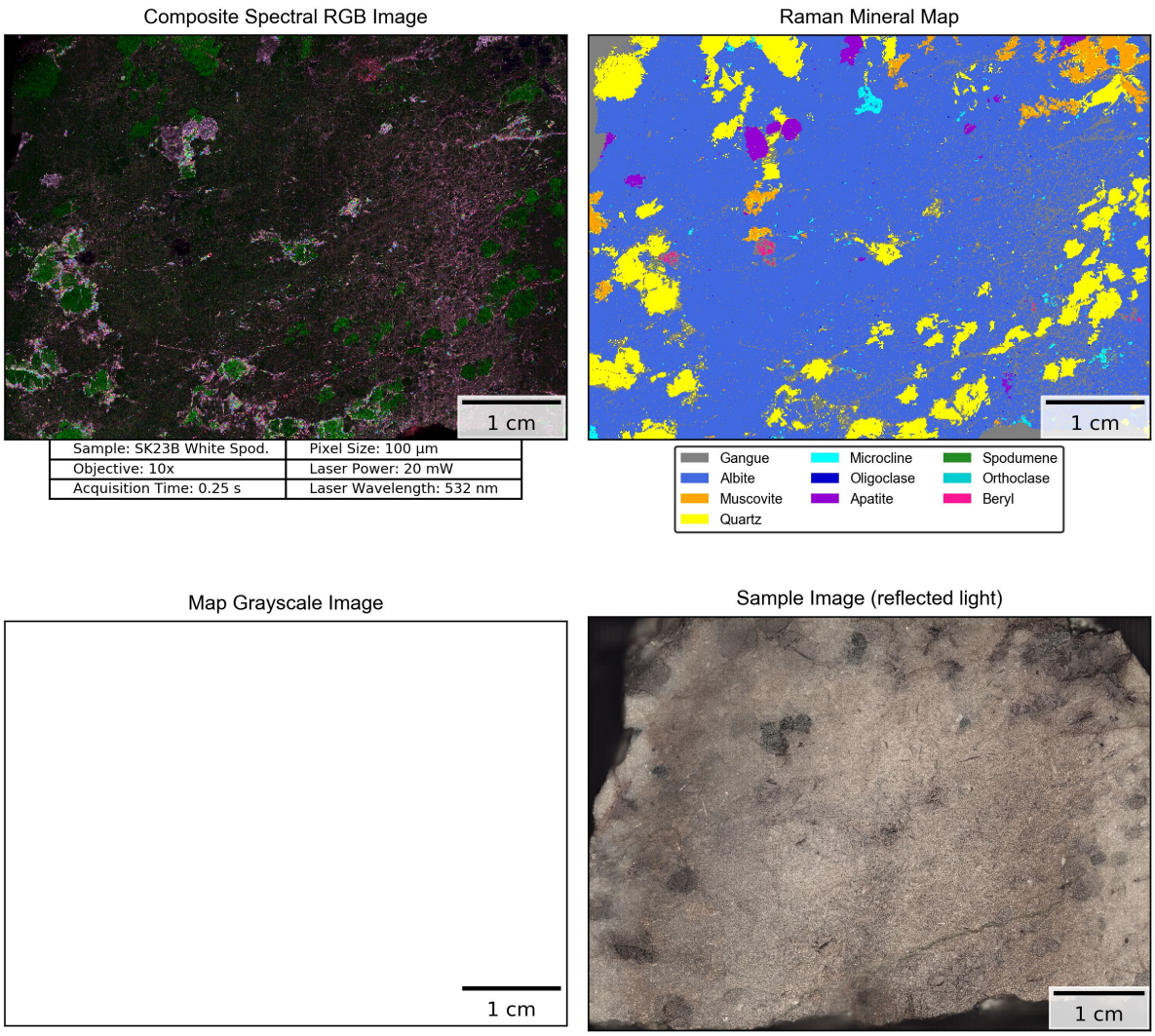

Figure 9. Raman analysis of sample **SK23B** spodumene

8.5 FTIR

Results are presented in **Figures 10-13**.

8.5.1 Hirvikallio Petalite

The petalite bulk sample, PHB, showed a petalite concentration of 58.6 wt%, with intermediate albite and quartz concentration and small amount of Spodumene.

Amongst the petalite crystal samples, PHC1, PHC2, PHC4 and PHH, the PHC4 showed the highest Petalite concentration at 95 wt%, with very low concentration of quartz and albite.

In Figure 8, all the samples are plotted, for the whole range as well as a focused area between 1300 – 400 cm^{-1}. In that focused area, a nominal albite spectrum is also included for comparison reasons.

As far as the petalite samples is concerned the spectral patterns are very similar between them, with differences manifesting the variability in the mineral content in each sample.

If one compares the PHH spectrum and the nominal albite, the two minerals have a very similar FTIR pattern. However, they are distinguishable in a mixture of other minerals.

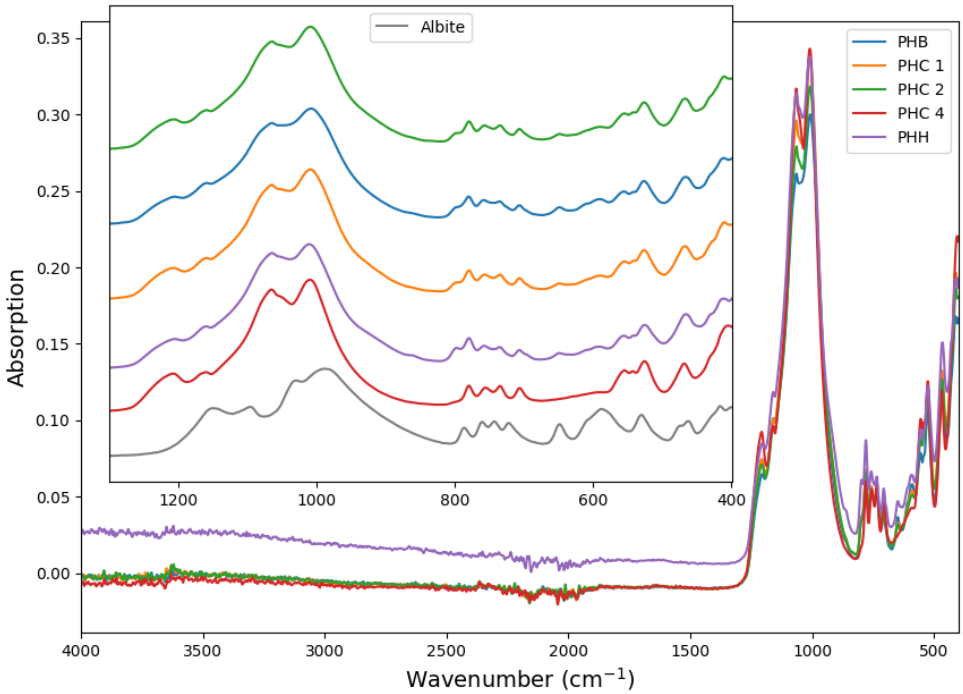

Figure 10. FTIR analysis of the Hirvikallio petalite.

8.5.2 Syväjärvi Green Spodumene

Spodumene varieties labelled as 'green', showed a similar pattern, Figure 9. Variations in the spectra are due to the different concentrations of Spodumene and the accessory minerals of albite, quartz, K-feldspar and muscovite.

The crystal samples separated from the bulk, SS19C and SS21C, did show higher concentration of spodumene, however with high concentrations of quartz and albite.

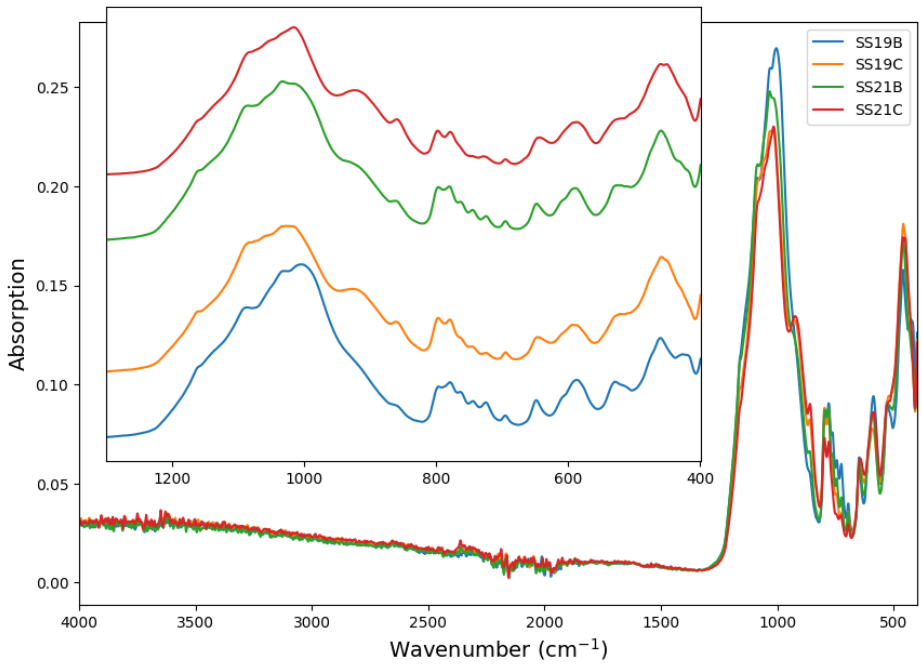

Figure 11. FTIR analysis of the Syväjärvi green spodumene

8.5.3 Länttä Pink Spodumene

Similarly, the pink spodumene bulk and crystal samples, in **Figure 10**, have some difference in their spectral pattern due to the concentration reduction of albite between bulk and crystal but also the increase of quartz in the crystal sample. (For XRD results see **Table 1).**

Between the green and the pink spodumene, not distinctive difference can be made, as all variations observed are within the context of the existing mineralogy, in this samples.

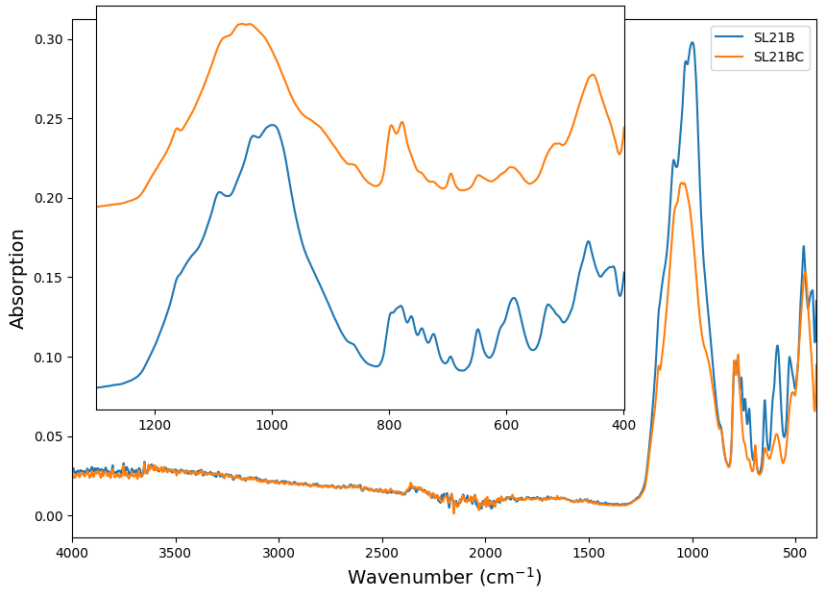

Figure 12. FTIR analysis of the Länttä pink spodumene

8.5.4 Kietyönmäki Spodumene

The **SK23B** sample shows a clear albite signal in the FTIR, as XRD as also quantified. A nominal spectrum of albite is also displayed for comparative purposes. Due to the very high concentration in albite at 77.3 wt%, quartz bands is almost discernible at e.g., 697 cm^{-1}, with spodumene not be able to identify without further spectra processing.

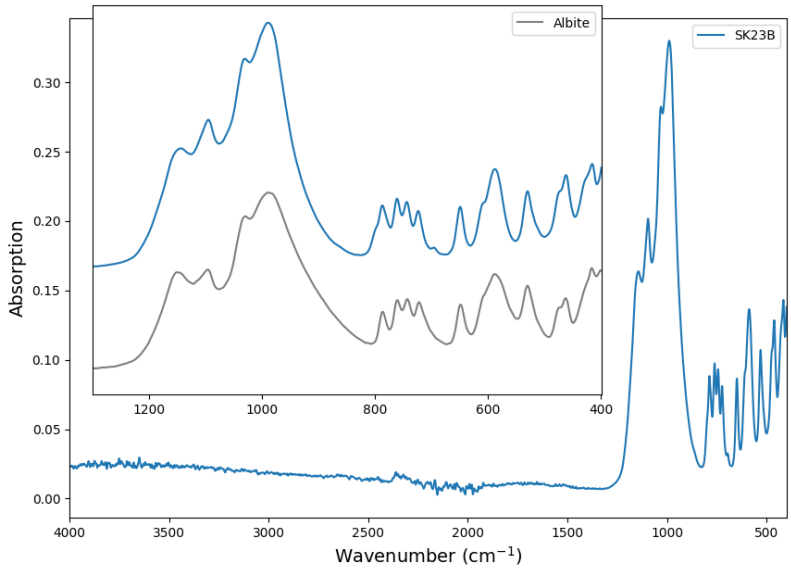

Figure 13. FTIR analysis of the Kietyönmäki spodumene

9. DISCUSSION

The samples have been characterized using the **META** multidisciplinary geomaterial workflow. This workflow has been developed by X-ray Mineral Services to explore various Mineralogical, Elemental and Textural Analyses (META) to provide cross-validated analytical data.

"Gold standard" techniques of XRD, ICP-OES/MS, Automated Mineralogy (AMICS) and Raman spectroscopy were used to characterise the samples, with subsequent calibration of FTIR, a portable technique.

9.1 Cross-validation of XRD and ICP results

A mass balance calculation was used to validate the mineral quantification given by the Rietveld method. Simplified mineral formulas have been used to calculate bulk chemical composition of the samples from the quantification of the minerals obtained by **XRD** and compared with the **ICP-OES** measured results. The scope of the mass balance calculation is to identify any discrepancies between the measured chemical composition of a sample and the mineral content. There is a very good correlation between the chemistry measured by ICP and the chemistry calculated using a mass balance calculation (**Figures 14** & **15**). The quantification of petalite and spodumene is accurate and the error in quantification is not greater than 2%. Mn, Ti, Fe and minor oxides are not shown in **Figure 14** for clarity because they are low in concentration and therefore not very relevant.

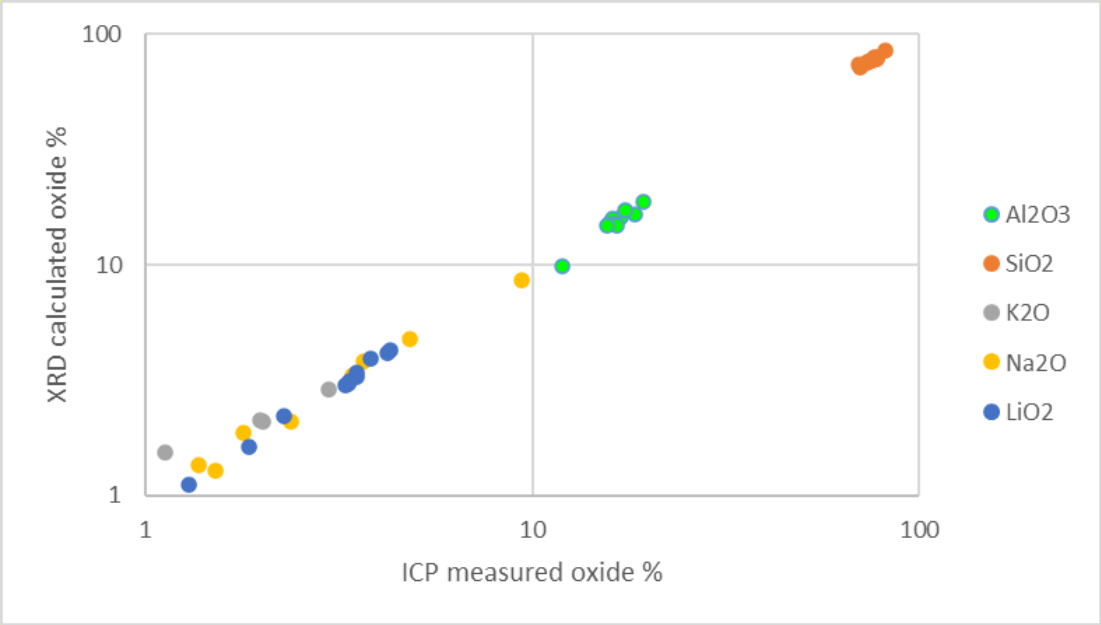

Figure 14. Measured vs. calculated chemistry. Good correlation between the two datasets demonstrates the accuracy of the XRD quantification.

Sample SS19B show a high Ce-content that is not explained with any minerals identified by **XRD**. A small amount of chlorite is present in many samples, in most of the cases is not quantifiable except for sample SL21C where is 2%. The 003 reflection for chlorite this sample is higher than in usual chlorite suggesting it

could be cookeite, but the evidence of cookeite being present is not enough to confirm it.

Beryl is also present, and the detection limit is very small (0.1%) making one of the minerals with lower detection limit by **XRD** (with this long scan).

Crystal 3 contains a clay mineral, most probably smectite, but unfortunately there was not enough material for clay fraction analysis. It also contains an unidentified mineral that is probably less than 1 or 2%.

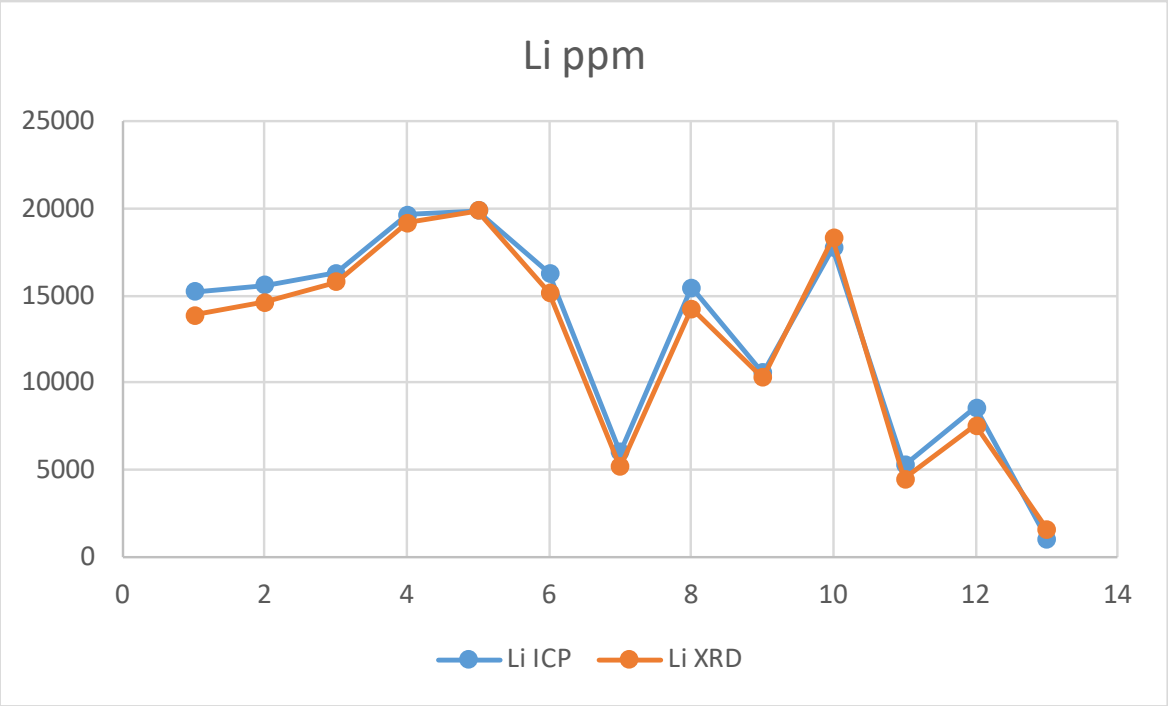

Figure 15. Comparison between lithium by ICP-OES and lithium by XRD (calculated from the mineralogy), according to sample analysed

9.2 Cross-validation of mineralogical results: XRD vs AMICS vs Raman

Mineralogical data acquired by automated mineralogy technique (**AMICS**) was compared and cross-validated with quantitative mineralogical data acquired by X-ray diffraction (**XRD**) analysis and qualitative data acquired by Raman spectroscopy. Given that the analyses were not conducted on the same sub-sample and appreciating the differences in analysis type (2D surface area vs. volumetric whole rock mass fraction), reconciliation is reasonable for the major and minor minerals. Some variance is expected due to the difference in sample splits and the fact that the AMICS and Raman analyses are conducted on a bulk sample and not on homogenised whole rock like XRD.

A total of eleven minerals were identified by XRD whereas AMICS was able to distinguish 14 different mineral

phases. The comparison between the XRD and AMICS results are illustrated in **Figures 15-17** for the samples with both datasets available. Identification of the mineral phases between the methods is well in agreement and only minor differences can be seen in the identification of minor and trace phases. A key difference is related to the identification of eucryptite (Li-Al-silicate) by AMICS while Raman and XRD have failed to do so. Eucryptite is found as a subordinate phase e.g., forming veinlets in spodumene (SL21B-1) but also appears together with quartz in the AMICS data while XRD results only indicate the presence of petalite and spodumene. **Eucryptite** is a mineral that can be easily distinguished by XRD in this rock-matrix and therefore it is likely that the areas classified as eucryptite by AMICS represent areas of the sample where cracks contain a residue of Al-oxide polishing compound. A sampling issue resulting in the lack of eucryptite in the XRD data cannot be completely ruled out, but because of the textural characteristics of the eucryptite, this is unlikely to be the case.

Moreover, AMICS has identified trace amounts of Fe-phosphate (SS21B-1) and zircon (SL21B-1, SK23B), which are not seen in the XRD data because of their low concentrations. On the contrary, trace amounts of smectite and amphibole were identified by XRD in samples PHB-1 and SS19B, respectively, but were not differentiated in the AMICS data. As the AMICS data expresses minerals in groups, small amounts of smectite are likely to be grouped with other minerals, e.g., chlorite. The presence of amphibole in the XRD data is likely related to a sampling bias with the XRD being more representative of the bulk mineralogy.

Large differences in the quantification of the major mineral phases can be seen in petalite, spodumene, quartz and plagioclase (**Figures 13** - **15**). Variations in the quantification of the main mineral phases are likely related to generic differences between the two techniques, and related sample preparation and sample representativity. XRD provides a quantitative and more accurate determination of minerals present in a bulk sample as it represents a homogenized whole rock sample. AMICS, in turn, examines discreet mineral particles in a polished two-dimensional grain mount giving emphasis on grain size. Therefore, the presence of large grains, e.g., spodumene and petalite, is readily overquantified/over-represented in the AMICS data. Where XRD is a bulk technique, AMICS is a microscopic technique. AMICS is very powerful in determining associations of specific minerals through imaging and generating loads of useful data about textural properties but can be sensitive to statistical errors caused by the relatively small number of particles that can be analysed. XRD cannot give the mapping capabilities of AMICS and is limited by a higher detection limit (generally 2–3%, depending on the matrix and mineralogy) meaning that XRD cannot detect minerals at low concentrations but removes many of the statistical difficulties. Despite of that, small amount of beryl was detected by XRD and confirmed by ICP analysis.

To summarize, XRD offers an accurate bulk mineralogical analysis but lacks the resolution to detect low concentrations and the ability to provide textural information. AMICS on the other hand, has no struggle with the analysis of low concentrations and offers textural characterization and data on mineral affinities, but yet, benefits from the external calibration of the XRD to validate the data. Nevertheless, each dataset should be considered reliable in its own right on the subsample which was analysed. Hence, these techniques should be considered complementary and used together.

Identification of certain mineral phases can further be enhanced using Raman spectroscopy. Acquired Raman spectra is determined by molecule-specific combinations of chemical bonds and hence founded on the

structure and chemistry of the analysed material. Consequently, mineral polymorphs, can be confidently differentiated and chemical variations within a mineral species can be detected. Raman spectroscopy, however, provides only qualitative information about the mineral phases present in the sample. The acquires Raman data is well in line with the XRD and AMICS data identifying the presence of major and minor petalite, spodumene, quartz, albite, K-feldspar, plagioclase and muscovite. Also, small amounts of beryl and apatite were identified.

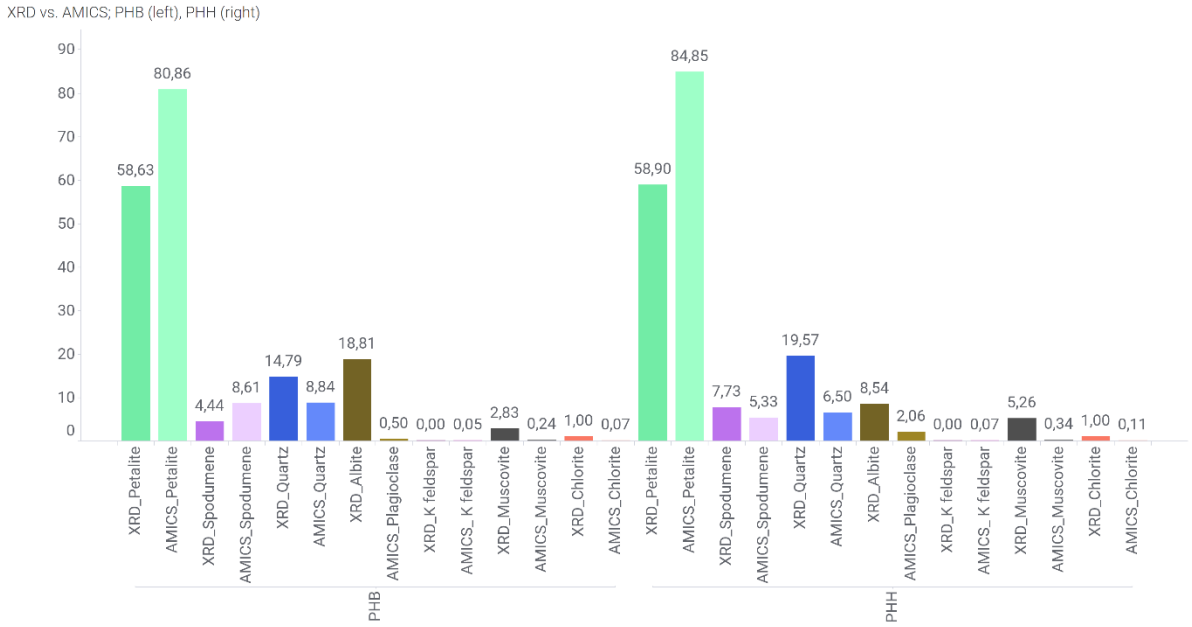

Figure 15. Comparison of the XRD mineralogy (bulk) with AMICS mineralogy (by area) for the major mineral groupings in samples PHB (left) and PHH (right).

December 11, 2023

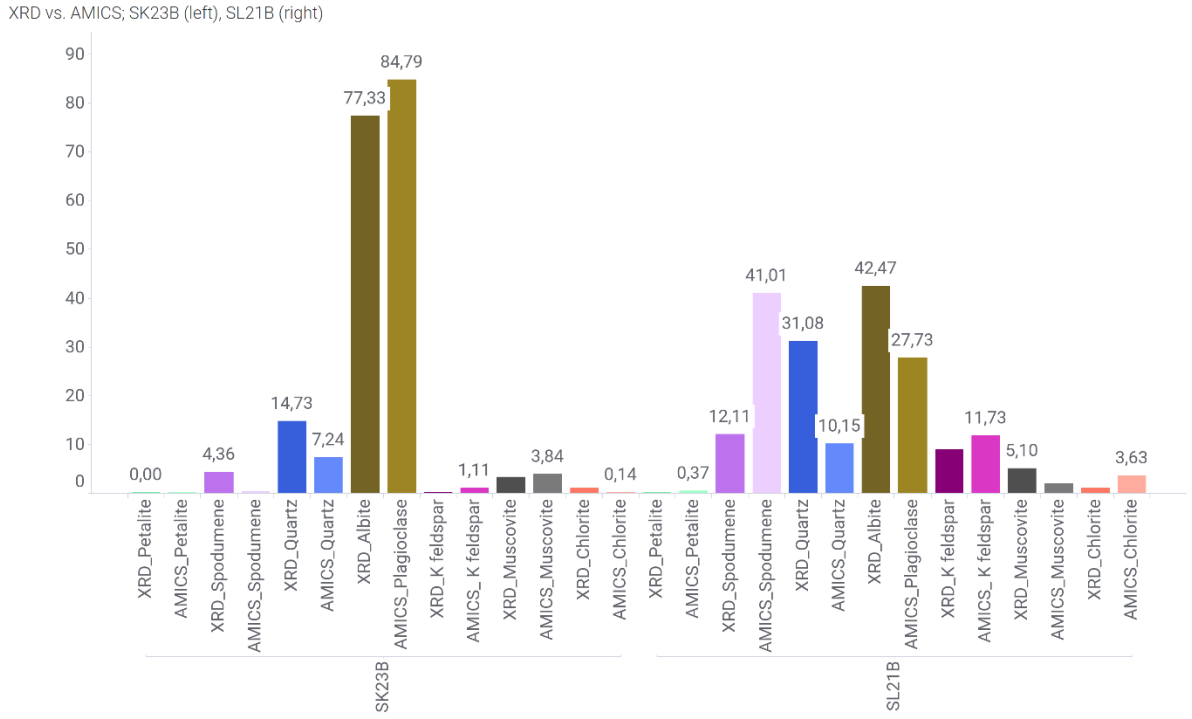

Figure 16. Comparison of the XRD mineralogy (bulk) with AMICS mineralogy (by area) for the major mineral groupings in samples SK23B (left) and SL21B (right).

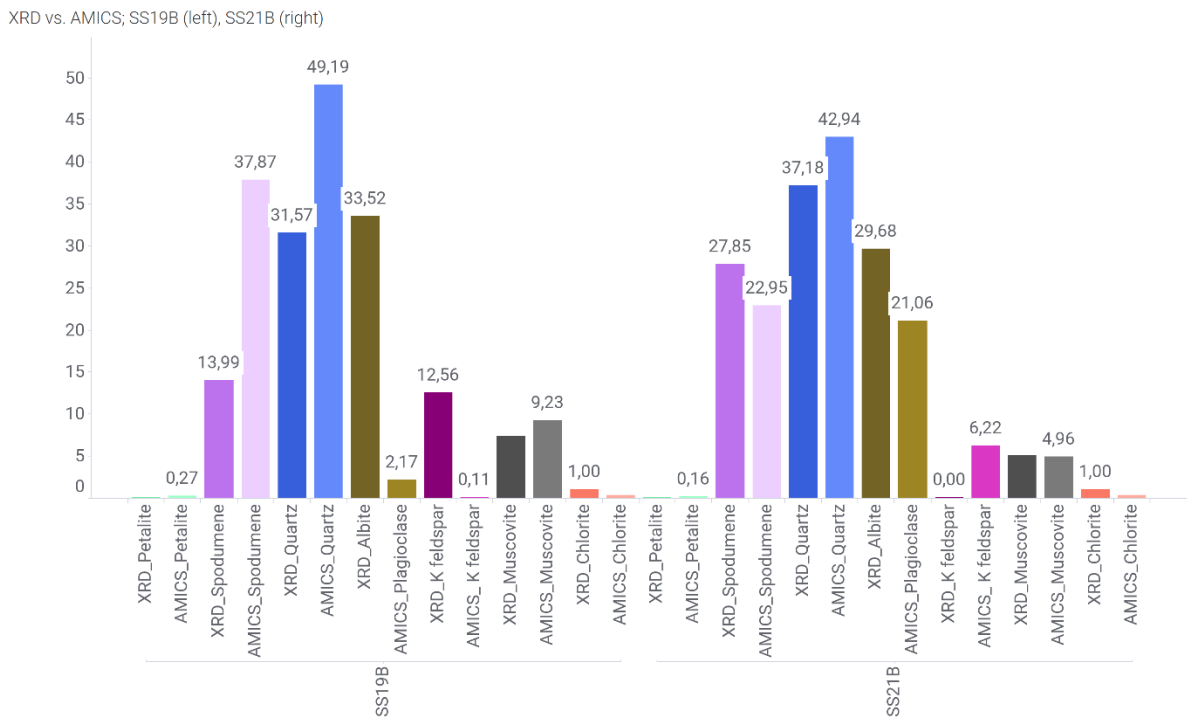

Figure 17. Comparison of the XRD mineralogy (bulk) with AMICS mineralogy (by area) for the major mineral groupings in samples SS19B (left) and SS21B (right).

As far as the Raman & AMICS comparison is concerned, both techniques cross-validate each other. As first Raman data were acquired and subsequently AMICS data on the same polished surface it was made possible to have surface overlapping on both techniques.

Detailed textural observation can be done with both techniques, although AMICS provide higher image resolution (inherent to X-ray spot size).

One potential disadvantage of Raman, is the non-direct identification of chlorite phases, as opposed to AMICS. Chlorite can be identified with higher retention time by Raman laser, yet in that study a much shorter time was selected. An example of Chlorite phase in Raman figures can be observed in sample SL21B, for pink spodumene, at the upper left corner for the RGB image and the mineral image. There is a region of brighter colours, and 'Gangue' mineral identified respectively.

We assess that in the case of Lithium-bearing minerals, Raman mapping and Raman spectral matching has a further potential as it can distinguish the major Li-bearing minerals, both in a laboratory-based technique (Raman microscopy) as well as develop portable solutions without the need of extra software for mineral calculation (e.g. AMICS).

10. CONCLUSION

Bulk analytical techniques such as **XRD** and **ICP** provide the "gold standard" methods for mineralogical and chemical analysis, particularly when used in conjunction with one another providing a more robust dataset. **XRD** has proven to provide accurate data for this type of samples specially when a high-resolution scan is used reducing the well-known problem of the limit of detection by **XRD**.

From a mineralogical and textural perspective both **Automated Mineralogy** and **Raman** microscopy were able to produce mineral maps of these rock types.

FTIR analysis revealed the spectral consistency of our samples for the **XRD** quantified mineralogy. Also, demonstrated that spodumene, petalite and albite can be distinguished well within a mixture of other mineral phases as well as themselves when these co-exist, within the **FTIR** detection limits for such minerals and matrices.

This being the case, it would be possible to build appropriate **XRD-FTIR** predictive modelling, which would take the **XRD** results as the dependent variable and the **FTIR** as the independent variable, with such models being used for quickly predicting petalite, spodumene, albite and quartz content using a portable **FTIR** machine on site / field during an exploration campaign.

11. ACKNOWLEDGEMENTS

The authors would like to thank **Duncan Pirrie** at Helford Geoscience Ltd and **Matt Power** at Vidence kindly provided the Automated Mineralogy results. **Business Finland** funded this study.

12. REFERENCES

Finlay, A. J., Wray, D. S., Comfort, G., & Moore, J. K. (2023).
Radioactive heat production variations in the Faroe-Shetland Basin: key new heat production, geological and geochronological data for regional and local basin modelling. ***Petroleum Geoscience***, Volume 29. https://doi.org/10.1144/petgeo2022-039

Jarvis, I., & Jarvis, K. E. (1992a).
Inductively coupled plasma-atomic emission spectrometry in exploration geochemistry. Journal of ***Geochemical Exploration***, 44(1-3), 139-200.

Jarvis, I., & Jarvis, K. E. (1992b).
Plasma spectrometry in the earth sciences: techniques, applications and future trends. ***Chemical Geology***, 95(1-2), 1-33.

Moore M. & Reynolds R. C. (1997).
X-ray Diffraction and the Identification and Analysis of Clay Minerals. ***Oxford University Press***.

Pirrie D. & Rollinson G.K. (2011).
Unlocking the application of automated mineralogy***.*** ***Geology Today***, 27, 226-235.

Post J. E. & Bish D. L. (1989).
Rietveld refinement of crystal structures using powder X-ray diffraction data. ***Mineralogical Society of America***, Review in Mineralogy, 20, 277-308.

Schultz B., Sandmann D. & Gilbricht S. (2020).
SEM-based automated mineralogy and its application in geo- and material sciences. ***Minerals***, 10, 1004; doi:10.3390/min10111004.

December 11, 2023

APPENDIX

December 11, 2023

Samples

Massive **petalite** from Hirvikallio, sample **PHB-1**

December 11, 2023

Massive **petalite**, **PHH 4.c.** from Hirvikallio

December 11, 2023

Green **spodumene**, Keliber Syväjärvi, Pilot 2019, sample **SS19B**

December 11, 2023

Green **spodumene**, Keliber Syväjärvi Nov 21, sample **SS11B-1**

December 11, 2023

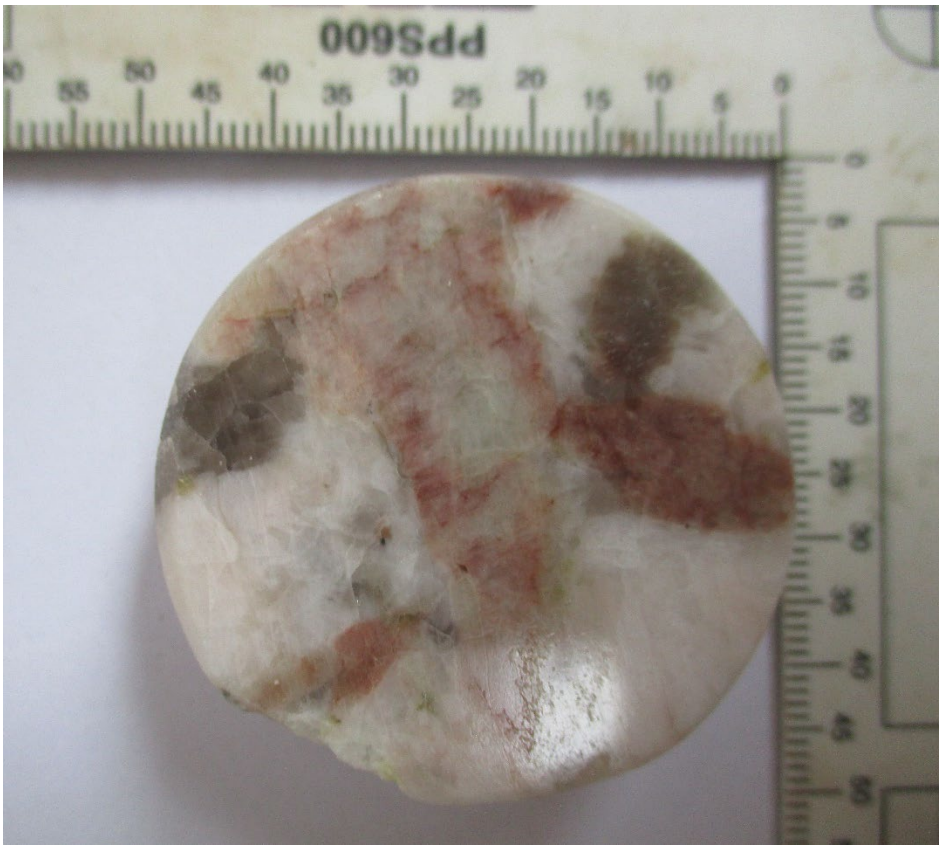

Pink **spodumene** Keliber Länttä, Nov 21, sample **SL21B-1**

December 11, 2023

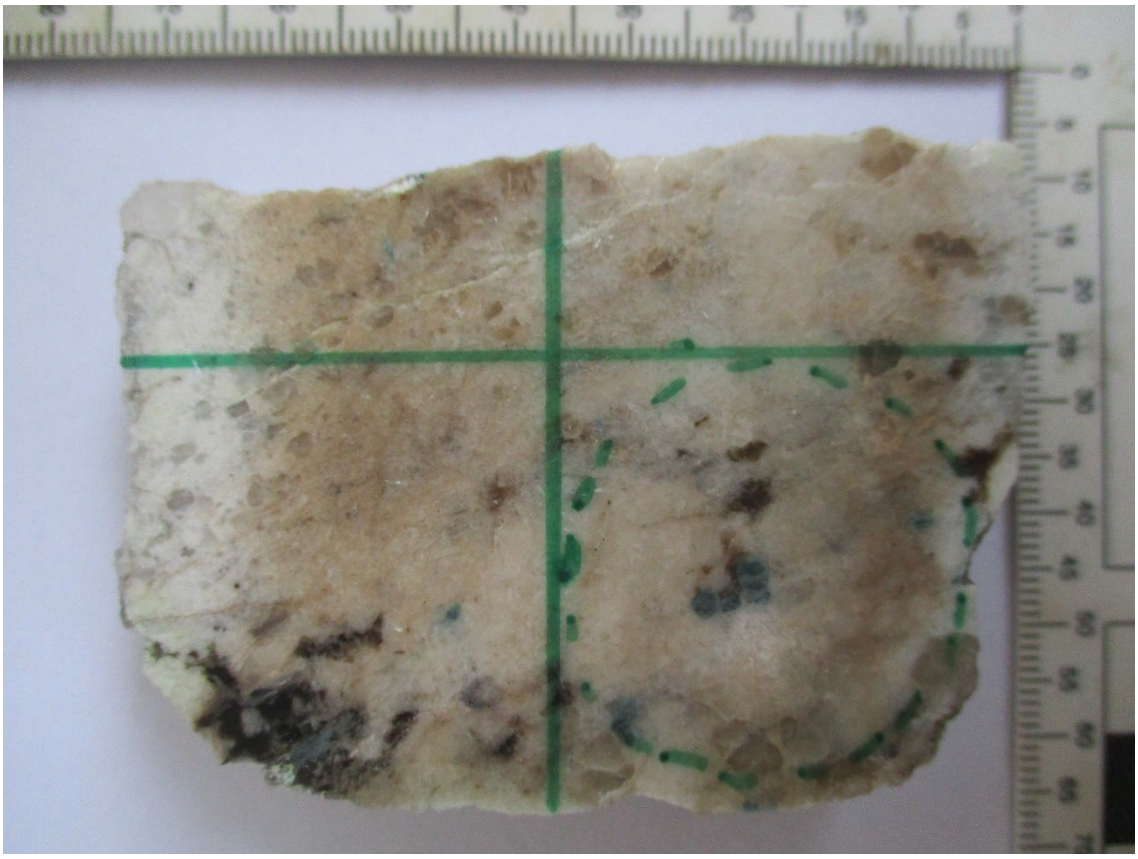

Spodumene from Kietyönmäki, sample **SK23B**

December 11, 2023

Further AMICS Images, Mineralogy & Textures

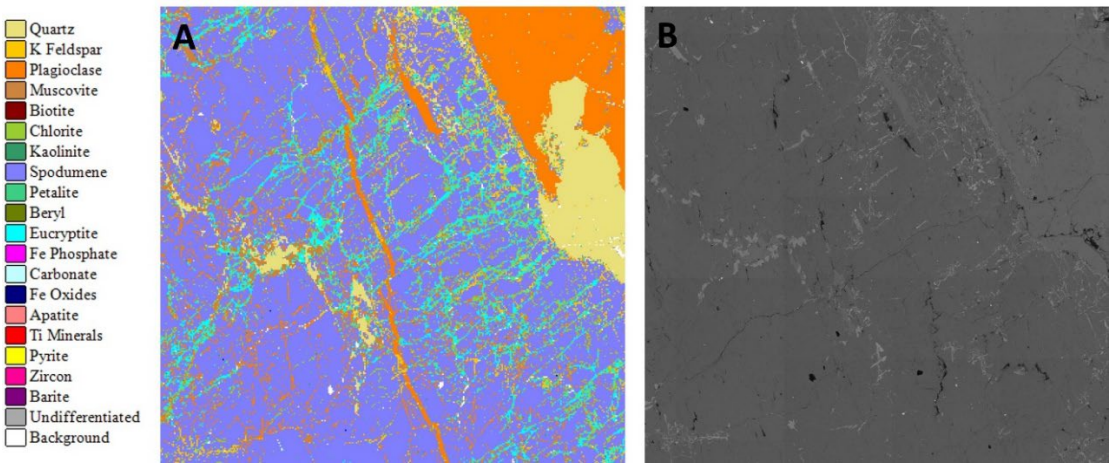

Further details of sample **SL21B-1**, pink spodumene, with AMICS image (A) and corresponding BSE image (B).

n

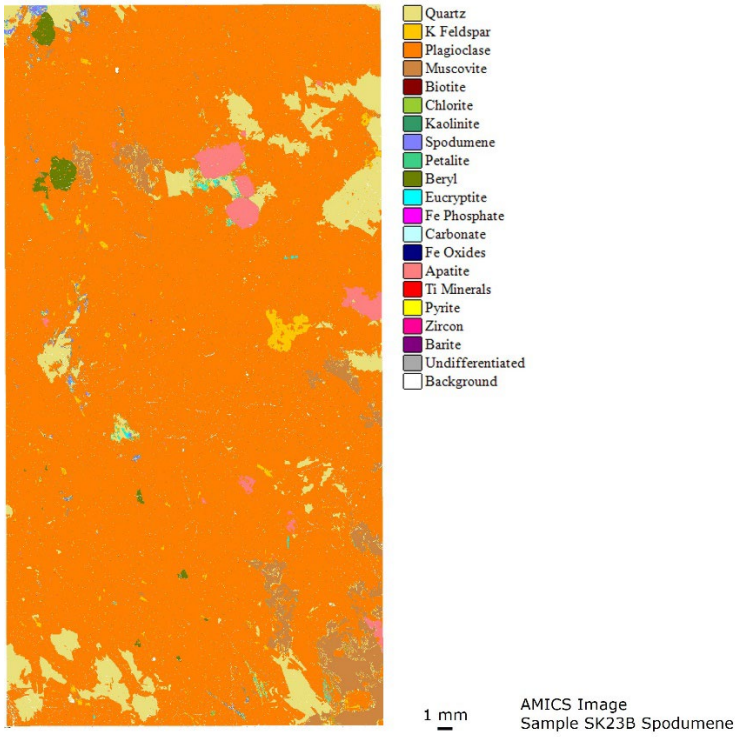

Sample **SK23B**, with ultra-trace spodumene present (See **Table 6**)

December 11, 2023

End of Report